Journal of Mathematical Chemistry, Vol. 43, No. 1, January 2008 (© 2007)
DOI: 10.1007/s10910-006-9187-5

Combinatorial enumeration of three-dimensional trees as stereochemical models of alkanes: an approach based on Fujita's proligand method and dual recognition as uninuclear and binuclear promolecules

Shinsaku Fujita

Department of Chemistry and Materials Technology, Kyoto Institute of Technology, Matsugasaki, Sakyoku, Kyoto 606-8585, Japan
E-mail: fujitas@chem.kit.ac.jp

Received June 20, 2006; accepted July 20, 2006

Three-dimensional (3D) trees, which are defined as a 3D extension of trees, are enumerated by Fujita's proligand method (Fujita, *Theor. Chem. Acc.* 113 (2005) 73–79 and 80–86; 115 (2006) 37–53). Such 3D-trees are dually recognized as uninuclear promolecules and as binuclear ones. The 3D-trees regarded as uninuclear promolecules are enumerated to give the gross number of 3D-trees, which suffers from redundancy due to contaminants. To evaluate the number of such contaminants, the 3D-trees are alternatively enumerated as binuclear promolecules. Cycle indices with chirality fittingness (CI-CFs) composed of three kinds of sphericity indices (SIs), i.e., a_d for homospheric cycles, c_d for enantiospheric cycles, and b_d for hemispheric cycles are obtained for evaluating promolecules of the two kinds. The CI-CFs for the uninuclear promolecules and those for the related binuclear promolecules are compared in terms of the dichotomy between balanced 3D-trees and unbalanced 3D-trees. Thereby, the redundancy due to such contaminants is deleted effectively so as to give the net number of 3D-trees. The validity of this procedure is proved in three ways, all of which are based on the respective modes of the correspondence between uninuclear promolecules and binuclear ones. In order to enumerate 3D-trees by following this procedure, the CI-CFs are converted into functional equations by substituting the SIs for $a(x^d)$, $c(x^d)$, and $b(x^d)$. Thereby, the numbers of 3D-trees or equivalently those of alkanes as stereoisomers are calculated under various conditions and collected up to 20 carbon content in a tabular form. Now, the stereochemical problems (on the number of stereoisomers) by van't Hoff (van't Hoff, *Arch. Néerlandaises des Sci. Exactes et Nat*, 9 (1874) 445–454) and by LeBel (Le Bel, *Bull. Soc. Chim. Fr.* (2), 22 (1874) 337–347) and the enumeration problems (on the number of trees) by Cayley (Cayley, *Philos. Mag.* 47 (1874) 444–446), both initiated in the 1870s, have been solved in a common theoretical framework, which satisfies both chemical and mathematical requirements.

KEY WORDS: alkane, stereoisomer, 3D-tree, enumeration, sphericity

1. Introduction

Since van't Hoff [1] and LeBel [2] founded stereochemistry in the 1870s, the enumeration of stereoisomers has been one of the central problems, as found by the fact that van't Hoff himself [1] already discussed the number of stereoisomers having n asymmetric carbons. In the same 1870s, on the other hand, combinatorial enumeration of trees as models of alkanes was initiated by a mathematician Cayley [3, 4]. Although Cayley already recognized such trees as models of isomers of alkanes [4], his work as well as most successive works on the combinatorial enumeration regarded isomers as graphs, not as three-dimensional (3D) objects (i.e., stereoisomers), as found in reviews [5–8] and books [9–12]. For example, Henze and Blair [13] reported the number of alkanes of a given carbon content, where the alkanes were regarded as graphs. Pólya [14, 15] applied his main theorem (Hauptsatz) to the evaluation of the number of trees as graphs by using alternating groups and symmetric groups. Although the use of the alternating groups was claimed to be capable of counting spatial isomers in terms of Pólya's treatment, it was conceptually impossible to distinguish between achiral stereoisomers and two enantiomers of chiral ones as well as to comprehend stereochemical problems on pseudoasymmetry and *meso*-compounds, as discussed in our recent papers [16–18]. Although Robinson et al. [19] has reported the enumeration of alkanes as stereoisomers by modifying Pólya's cycle indices (CIs), it is still desirable to develop a more systematic method for comprehending the stereochemical problems.

In the enumeration of stereoisomers (more generally than alkanes or trees as 3D-objects), the non-rigidity of skeletons for deriving such stereoisomers makes it difficult to recognize congruence between two stereoisomers. Because free rotations around bonds (edges) cause multiple (or in fact infinite) conformational changes, it is obviously impossible to compare such multiple or infinite number of conformers. To avoid this type of difficulty, we have proposed the concepts of *proligands* and *promolecules* [20–22], by which the multiple or infinite number of conformers can be replaced by a single promolecule without conformational changes and the symmetries of the conformers can be limited within the point-group symmetry of the promolecule.

Even though the difficulty due to multiple conformational changes is avoided by introducing the concepts of proligands and promolecules, there exists a further difficulty which stems from the inner structures of stereoisomers as 3D-objects. This type of difficulty is closely related to the stereochemical problems on pseudoasymmetry and *meso*-compounds. To avoid the difficulty, we have developed the USCI (unit-subduced-cycle-index) approach by means of algebraic derivation [23–26] as well as by means of a diagrammatical formulation [27–29]. The crux of Fujita's USCI approach is the concept of *sphericities of orbits* governed by coset representations.

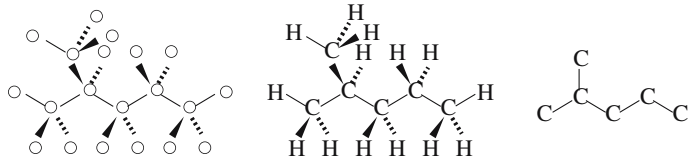

1 **2** **3**

Figure 1. 3D-Trees of various expressions. A 3D-tree with vertices and edges (**1**), a full expression as an alkane (**2**), and a carbon-skeletal expression as an alkane (**3**).

By the integration of the concepts of proligands and promolecules [20–22] and the concept of sphericities [23], we have recently proposed *the proligand method* for enumerating stereoisomers [16–18]. To accomplish the enumeration of alkanes, the nested nature appearing in the structures of alkanes should be investigated by extending the proligand method.

The present paper is devoted to the enumeration of three-dimensional trees (3D-trees) as models of alkanes. Thus, such 3D-trees formulated by using the concepts of proligands and promolecules will be discussed in terms of dual recognition as uninuclear and binuclear promolecules. Thereby, 3D-trees will be categorized into balanced and unbalanced 3D-trees, the numbers of which will be evaluated distinctly by using generating functions based on Fujita's proligand method.

2. Characterization of 3D-trees as promolecules

2.1. 3D-trees and alkanes

A 3D-tree is defined as a 3D version of a tree, which is in turn defined usually as a graph having v vertices and e edges, where they satisfy the relationship $v = e + 1$. Various expressions of such 3D-trees are shown in figure 1, where the degree of each non-terminal vertex is presumed to be equal to 4 in accord with the tetravalency of a carbon atom.

The first formula (**1**) expresses a 3D-version of a usual tree, where each vertex is represented by an open circle and each edge is represented by a wedge, a boldface hashed line, and a straight line to show the configuration of each non-terminal vertex. The term *configuration* comes from a chemical origin to denote a spatial arrangement around a vertex. In accord with chemical conventions, each wedge denotes an edge (bond) situated in the front side out of the page, each boldface hashed line denotes an edge (bond) situated in the back side of the page, and each straight line denotes an edge (bond) laid in the page. The second formula (**2**) shows the chemical counterpart of **1**, where each non-terminal vertex is regarded as a carbon atom and each terminal vertex is regarded as a hydrogen atom. This formula expresses 2-methylpentane, which is one of alkanes

of carbon content 6. The third formula (**3**) expresses the carbon-skeleton of **2**. In this formula, the configuration of each carbon center is not expressed explicitly because it is unnecessary to this case.

Throughout this paper, carbon-skeletal expressions of the third type are employed where a wedge, a boldface hashed line, and/or a straight line are used to show the configuration of each non-terminal vertex if necessary. For the sake of simplicity, such carbon-skeletal expressions are referred to as 3D-trees in a mathematical context and as alkanes in a chemical context.

2.2. 3D-trees as uninuclear and binuclear promolecules

By applying the concepts of proligands and promolecules [20–22] to 3D-trees, two type of promolecules, i.e., uninuclear promolecules and binuclear promolecules, can be simultaneously or dually ascribed to a 3D-tree, because each 3D-tree is composed of vertices and edges.

A given 3D-tree is regarded as a uninuclear promolecule when an appropriate vertex is selected as a nucleus (•). For example, the 3D-tree (**3**) is regarded as a uninuclear promolecule if the non-terminal vertex denoted by a solid circle (•) is selected as a nucleus, as shown in **3a** (figure 2). By extracting the non-terminal vertex (denoted by a solid circle • as a nucleus) and its adjacent vertices (denoted by open circles ∘ as substitution positions), we obtain **4** as a uninuclear skeleton, where two open circles are added to treat null terminal vertices (chemically hydrogen atoms). The extracted skeleton having four substitution positions is a 3D-object belonging to a point group, as shown in **4** (e.g., $\mathbf{T}_d$ for a tetrahedral skeleton). During this process, there appear two planted 3D-trees **5** (an isopropyl ligand) and **6** (an ethyl ligand) as well as two trivial planted 3D-trees (•—∘). After they are regarded as achiral proligands (X and Y), we obtain the corresponding promolecule (**7**). It should be noted that the presence of null vertices (chemically hydrogen atoms) plays a critical role if configurations are taken into consideration.

A given 3D-tree is alternatively regarded as a binuclear promolecule when an appropriate edge is selected as a binucleus. The term *binucleus* is here coined to denote an edge with two vertices. For example, the 3D-tree (**3**) is alternatively regarded as a binuclear promolecule if the adjacent non-terminal vertices denoted by open circles (∘) are selected as a binucleus, as shown in **3b** (figure 2). By extracting the non-terminal vertices (∘) (as substitution positions), we obtain a binuclear skeleton **8**. The extracted skeleton having two substitution positions is a 3D-object belonging to a point group ($\mathbf{D}_{\infty h}$ or its factor group $\mathbf{D}_{\infty h}/\mathbf{C}_{\infty}$). During this process, two 3D-planted trees **9** and **10** appear as substituents. After they are regarded as achiral proligands (X and Z), we obtain the corresponding binuclear promolecule (**11**).

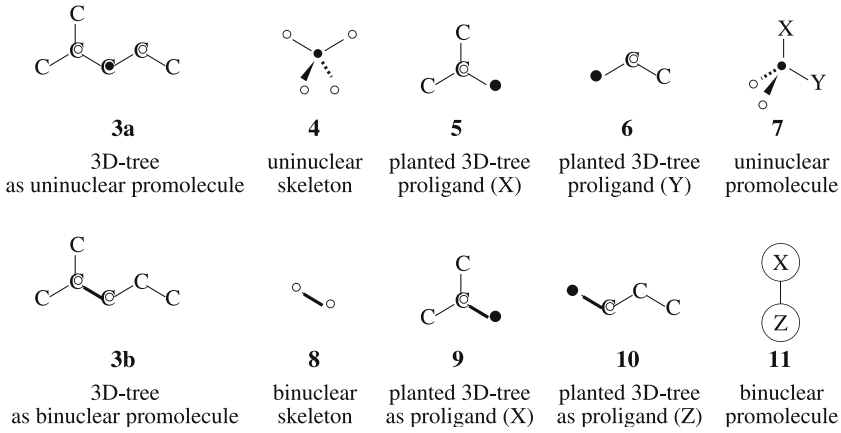

Figure 2. Dual recognition of a 3D-tree (**3**) as a uninuclear promolecule (**3a** or **7**) and a binuclear one (**3b** or **11**).

Both the uninuclear promolecule (**7**) and the binuclear promolecule (**11**) correspond to a single 3D-tree **3**. The dual recognition via **3a** and **3b** are different only in the criteria of selection, i.e., a vertex or an edge. However, the congruence between the uninuclear promolecule (**7**) and the binuclear one (**11**) cannot be formulated within equivalency due to point-group symmetries ($\mathbf{T}_d$ versus $\mathbf{D}_{\infty h}$). It is the next task to develop a methodology to formulate such congruence as untreatable by point-group symmetries.

2.3. Congruence between uninuclear promolecules and binuclear ones

To make such congruence treatable, let us apply the procedure described in figure 2 to every vertices and every edges in the 3D-tree (**3**). The resulting uninuclear and binuclear promolecules are listed in figure 3. Because equivalent vertices generate uninuclear promolecules equivalent under the action of the automorphism group of the relevant skeletons (e.g., $\mathbf{G} = \mathbf{T}_d$), the resulting uninuclear promolecules are regarded as being equivalent so as to be depicted as a single uninuclear promolecule. For example, the promolecule **17** (corresponding to **12**) is derived from the tetrahedral skeleton shown in **30** by placing p on position 1 and null ligands (or hydrogen atoms) on positions 2–4 as substituents. If we select the other vertex equivalent to the nucleus for **17** (i.e., the vertex incident to the wedge-shaped edge), a promolecule equivalent to **17** is generated. The other promolecules (**13**–**16**) generated by other modes of substitution should be regarded as being equivalent to **17**, although they are not superposable under the action of $\mathbf{T}_d$.

Suppose that uninuclear promolecules, the number of which is equal to u^*, are so equivalent (congruent) as to be regarded as a single 3D-object and

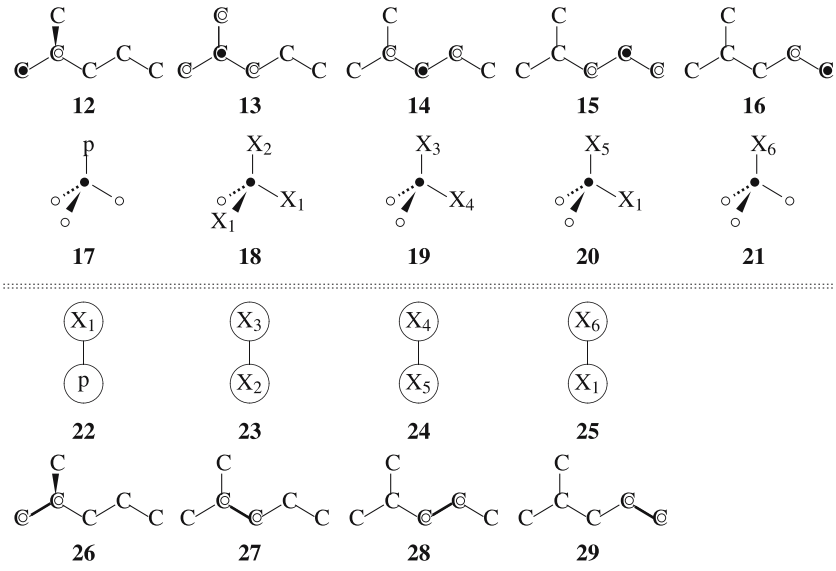

Figure 3. Uninuclear 3D-trees (**12**–**16**) and binuclear 3D-trees (**26**–**29**) as well as uninuclear promolecules (**17**–**21**) and binuclear promolecules (**22**–**25**) for characterizing an unbalanced 3D-tree (**3**).

to be counted just once in stereoisomer enumeration. To discuss the congruence between such uninuclear promolecules as relevant to a single 3D-tree, the first approach described in this section does not use their automorphism groups explicitly, but, instead, use the correspondence between uninuclear promolecules and binuclear promolecules.

It should be noted that the promolecule **17** (corresponding to **12**) contains a chiral proligand p (i.e., an *R*-1-methyl-1-butyl ligand or *R*-$CH(CH_3)CH_2CH_2CH_3$). Because the nucleus selected (i.e., the terminal methyl vertex) in **17** is the same as the other methyl contained in p, the uninuclear promolecule **17** is globally regarded as being achiral (cf. **3**). Thus, there are cases in which an achiral promolecule has a chiral proligand if it is regarded as a uninuclear promolecule. Because the present treatment counts a pair of enantiomers just once, the proligand p is depicted as a representative of a pair of p and its enantiomer proligand ($\overline{p}$).

From a viewpoint of combinatorial enumeration, the uninuclear promolecules (**17**–**21**) are generated from the skeleton (**30**) by placing four substituents selected from a set of proligands:

$$\mathbf{X} = \{p, X_1, X_2, X_3, X_4, X_5, X_6\}, \tag{1}$$

where we place

$$\begin{aligned} p\ (\overline{p}) &= R/S\text{-}CH(CH_3)CH_2CH_2CH_3, \quad x^5, \\ X_1 &= CH_3, \quad x, \end{aligned}$$

$$\begin{aligned} X_2 &= CH_2CH_2CH_3, & x^3,\\ X_3 &= CH(CH_3)_2, & x^3,\\ X_4 &= CH_2CH_3, & x^2,\\ X_5 &= CH_2CH(CH_3)_2, & x^4,\\ X_6 &= CH_2CH_2CH(CH_3)_2, & x^5. \end{aligned}$$

When the carbon content of each proligand is taken into consideration, the uninuclear promolecules (**17**) is characterized by the term $x \times (x^0)^3 \cdot x^5$ $(=x^6)$ because of the presence of three null proligands (i.e., hydrogen atoms) and the proligand p (x^5); the uninuclear promolecules (**18**) is characterized by the term $x \times x^0 \cdot x^2 \cdot x^3$ $(=x^6)$ because of the presence of one null proligand and two proligands X_1 (x) and X_2 (x^3); the uninuclear promolecules (**19**) is characterized by the term $x \times (x^0)^2 \cdot x^3 \cdot x^2$ $(=x^6)$ because of the presence of two null proligands and two proligands X_3 (x^3) and X_4 (x^2); the uninuclear promolecules (**20**) is characterized by the term $x \times (x^0)^2 \cdot x \cdot x^4$ $(=x^6)$ because of the presence of two null proligands and two proligands X_1 (x) and X_5 (x^4); and finally the uninuclear promolecules (**21**) is characterized by the term $x \times (x^0)^3 \cdot x^5$ $(=x^6)$ because of the presence of three null proligands and the proligand X_6 (x^5). Thus, they are characterized by the term x^6 in accord with their carbon content 6. Because the uninuclear promolecules (**17**–**21**) represent a single 3D-tree (**3**), they should be counted just once (figure 4).

Let G_k be the number of uninuclear promolecules of carbon content k, where the automorphism group $\mathbf{G}(= \mathbf{T}_d$ in this case) is taken into consideration. The corresponding counting series is represented as follows:

$$G(x) = \sum_{k=1}^{\infty} G_k x^k. \tag{2}$$

Then the generating function $G(x)$ is evaluated by using the automorphism group $\mathbf{G}(= \mathbf{T}_d$ in this case). As found easily in figure 3, a single 3D-tree (e.g., **3**) corresponds to u^* of uninuclear promolecules, which are counted separately so as to contribute to the value G_k.

On the other hand, binuclear promolecules generated from equivalent edges as binuclei are equivalent under the action of the automorphism group of the

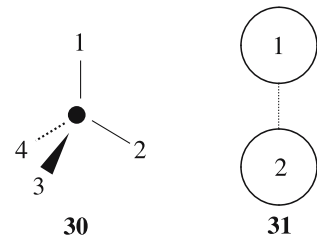

Figure 4. Uninuclear and binuclear skeletons.

relevant skeleton (e.g., $\mathbf{D}_{\infty h}$ or $\mathbf{D}_{\infty h}/\mathbf{C}_{\infty}$). According to their equivalency, they should be be depicted as a single binuclear promolecule. For example, the promolecule **22** (corresponding to **26**) is derived from the binuclear skeleton shown in **31** by placing X_1 on position 1 and p on position 2 as substituents. Another promolecule generated by another mode of placing the substituents are regarded as being equivalent to **22** under the action of $\mathbf{D}_{\infty h}$ (or $\mathbf{D}_{\infty h}/\mathbf{C}_{\infty}$). Even if we select the other edge equivalent to the binuclear for **22** (i.e., the wedge-shaped edge in **26**), a promolecule equivalent to **22** is generated so that the same situation holds true. By placing proligands selected from the set **X** (equation 1) on the vertices of the binuclear skeleton (**31**), we obtain b^* promolecules (**22**–**25**), which are so equivalent as to be regarded as a single 3D-object and to be counted just once in stereoisomer enumeration.

The binuclear promolecules (**22**–**25**) are generated from the skeleton (**31**) by placing two substituents selected from the same set of proligands as shown in equation 1. Let C_k be the number of 3D-trees of carbon content k. The corresponding counting series is represented as follows:

$$C(x) = \sum_{k=1}^{\infty} C_k x^k \tag{3}$$

Then the generating function $C(x)$ is evaluated by using the automorphism group $\mathbf{D}_{\infty h}$ (or $\mathbf{K} = \mathbf{D}_{\infty h}/\mathbf{C}_{\infty}$). As found easily in figure 3, a single 3D-tree (e.g., **3**) corresponds to b^* of binuclear promolecules, which are counted separately. The number b^* contributes to the coefficient C_k.

The comparison between the uninuclear promolecules (**17**–**21**) and the binuclear promolecules (**22**–**25**) indicates that they are generated by using the same set of proligands, i.e., **X** (equation 1). This situation holds true in general, because the two proligands of each binuclear promolecule appear in either of the relevant uninuclear promolecules:

Theorem 1. The set of uninuclear promolecules corresponding to a given 3D-tree and the relevant set of binuclear promolecules are generated by using the same set of proligands.

This theorem is effective especially in cases of containing chiral proligands. For example, the congruence between **17** and **22** can be determined even with the presence of the chiral ligand p.

2.4. The dichotomy of balanced and unbalanced 3D-trees

The first approach to discuss the congruence between such uninuclear promolecules as corresponding to a single 3D-tree is based on the value $u^* - b^*$, which is evaluated by the correspondence between the uninuclear promolecules and the relevant binuclear ones.

2.4.1. Balance-edges and balanced 3D-trees

To discuss the relationship between uninuclear promolecules and binuclear promolecules, we shall define a balance-edge as follows:

Definition 1 (Balance-edge). A balance-edge of a given 3D-tree is defined as an edge in which the planted tree (or proligand) at one terminal vertex is congruent to the planted tree (or proligand) at the other terminal vertex.

Edges other than a balance-edge in a given 3D-tree are called *slant-edges*.

Obviously, a balance-edge is contained in a binuclear promolecule which is represented by X–X, p–p ($\overline{p}$–$\overline{p}$), or p–$\overline{p}$, where X represents an achiral ligand; and p and $\overline{p}$ represent an enantiomeric pair of chiral proligands. On the other hand, a slant-edge is contained in a binuclear promolecule which is represented by X–Y, X–p, or p–q, where X and Y represents achiral ligands; and p and q represent chiral proligands.

A 3D-tree contains at most one balance-edge, because the inconsistency would occur if two or more balance-edges are present in the 3D-tree. This means that the presence/absence of such a balance-edge provides a criterion for classifying 3D-trees. Thereby, 3D-trees are classified into two categories:

Definition 2 (Balanced and unbalanced 3D-trees).

1. A balanced 3D-tree is defined as a 3D-tree having a balance-edge.
2. An unbalanced 3D-tree is defined as a 3D-tree which has no balance-edge.

According to the dichotomy described in definition 2, the enumeration of balanced 3D-trees and that of unbalanced 3D-trees are examined distinctly.

It should be emphasized that whether a given 3D-tree is balanced or not can be determined only by examining it as a binuclear promolecule. According to the types of balance-edges, such binuclear promolecules as X–X, p–p ($\overline{p}$–$\overline{p}$), or p–$\overline{p}$ are taken into consideration as balanced 3D-trees. Several examples of balanced trees of carbon content 8 are collected in figure 5, which contains a 3D-tree of *meso*-type (**36**).

Before we start the enumeration of balanced 3D-trees, we shall examine 2,3-dimethylhexane (**32**) as a typical example of balanced trees. The corresponding uninuclear and the binuclear promolecules are shown in figure 6. After the nuclei are selected as shown by the formulas **37**–**39**, the corresponding uninuclear promolecules **40**–**42** are constructed. Let u^* be the number of such uninuclear promolecules.

On the other hand, by selecting the binuclei as shown by the formulas **46**–**48**, the corresponding binuclear promolecules **43**–**45** are constructed. Let b^* be the number of such binuclear promolecules.

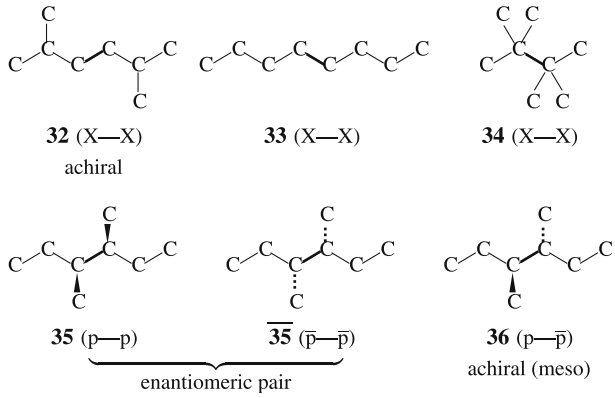

Figure 5. Balance-edges and balanced 3D-trees or alkanes. Each thick line denotes a balance-edge.

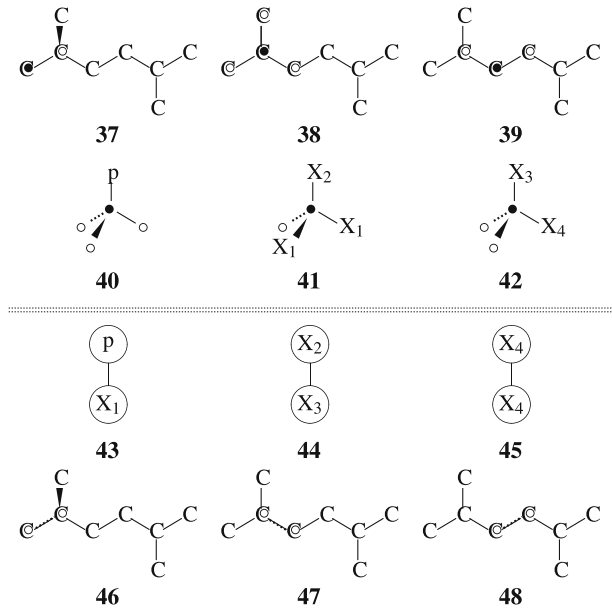

Figure 6. Uninuclear 3D-trees (**37**–**39**) and binuclear 3D-trees (**46**–**48**) as well as uninuclear promolecules (**40**–**42**) and binuclear promolecules (**43**–**45**) for characterizing a balanced 3D-tree (**32**).

Because they represent a single balanced 3D-tree, the contribution of the uninuclear promolecules (**40**–**42**) to the number of unbalanced 3D-trees should be zero, even though the contribution of the uninuclear promolecules (**40**–**42**) to the coefficient G_k is one or more, i.e., u^*. This implies that $u^* - b^* = 0$ for balanced trees.

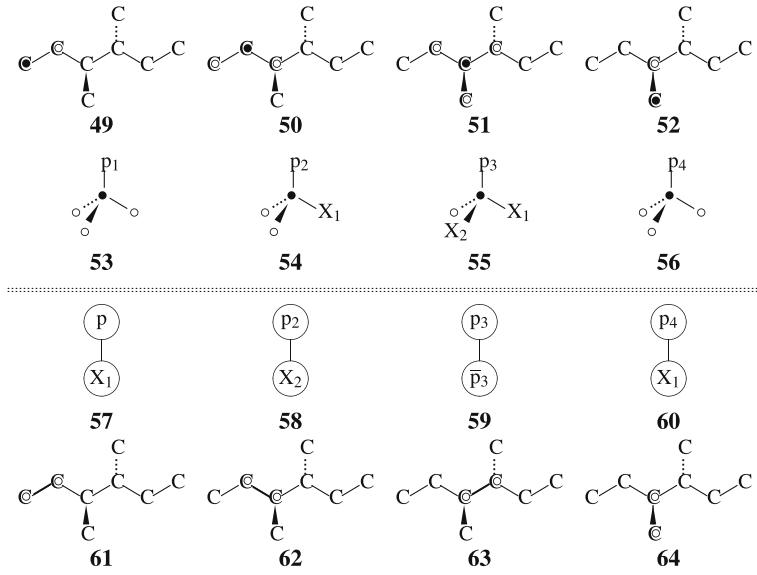

Figure 7. Uninuclear 3D-trees (**49**–**52**) and binuclear 3D-trees (**61**–**64**) as well as uninuclear promolecules (**53**–**56**) and binuclear promolecules (**57**–**60**) for characterizing a balanced 3D-tree (**36**).

Instead, one can find easily that only **45** is used to evaluate the number of balanced trees, although the coefficient C_k is used to evaluate the number (b^*) of the binuclear promolecules (**43**–**45**).

Let us next examine 3,5-dimethylhexane (**36**) as an example of balanced trees of *meso*-type. The corresponding uninuclear and the binuclear promolecules are shown in figure 7. After the nuclei are selected as shown by the formulas **49**–**52**, u^* of the corresponding uninuclear promolecules **53**–**56** are constructed. On the other hand, by selecting the binuclei as shown by the formulas **61**–**64**, b^* of the corresponding binuclear promolecules **57**–**60** are constructed.

The discussion described for the case shown in figure 6 is also effective to the case shown in figure 7. Because they represent a single balanced 3D-tree, the contribution of the uninuclear promolecules (**53**–**56**) to the number of unbalanced 3D-trees should be zero, even though the contribution of the uninuclear promolecules (**53**–**56**) to the coefficient G_k is one or more, i.e., u^*. This implies that $u^* - b^* = 0$ for balanced trees of *meso*-type. Instead, one can find easily that only **59** is used to evaluate the number of balanced trees, although the coefficient C_k is used to evaluate the number of the binuclear promolecules (**57**–**60**).

As found in the discussions described above for balanced 3D-trees, the number (u^*) of inequivalent uninuclear promolecules is equal to the number of inequivalent vertices and the number (b^*) of inequivalent binuclear promolecules is equal to the number of inequivalent edges. When balanced 3D-trees are taken into consideration, the cleavage at the balance-edge results in two equal

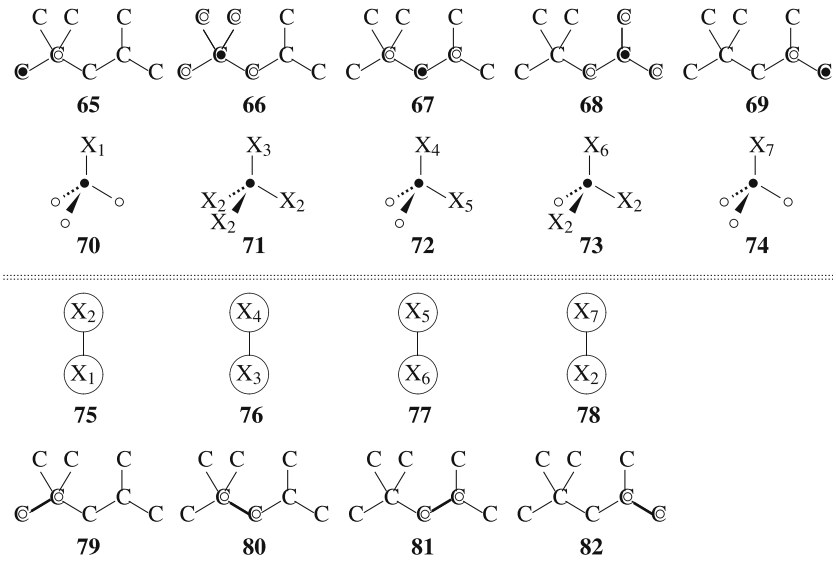

Figure 8. Uninuclear 3D-trees (**65**–**69**) and binuclear 3D-trees (**79**–**82**) as well as uninuclear promolecules (**70**–**74**) and binuclear promolecules (**75**–**78**) for characterizing an unbalanced 3D-tree.

halves, one of which is a sub-3D-tree containing all of the inequivalent vertices (the number u^*) and all of the inequivalent edges other than the balance-edge (the number $b^* - 1$). Hence, $u^* = (b^* - 1) + 1$. Thus, in any balanced 3D-tree, the number (u^*) of inequivalent vertices is equal to the number (b^*) of inequivalent edges. This is rewritten with respect to the relationship between uninuclear promolecules and binuclear promolecules relevant to a single balanced 3D-tree, giving the following theorem:

Theorem 2. As for any balanced 3D-tree, the number (u^*) of relevant uninuclear promolecules is equal to the number (b^*) of relevant binuclear promolecules. Hence, $u^* - b^* = 0$.
Theorem 2 is exemplified by figures 6 and 7.

2.4.2. Unbalanced 3D-trees

The 2-methylpentane as a 3D-tree (**3**) shown in figures 2 and 3 is an unbalanced 3D-tree, because it has no balance-edge. The number (u^*) of inequivalent uninuclear promolecules and the number (b^*) of inequivalent binuclear promolecules satisfy the relation $u^* - b^* = 5 - 4 = 1$, as shown in figure 3.

2,2,4-Timethylpentane shown in figure 8 is an unbalanced 3D-tree, because it has no balance-edge. The number (u^*) of inequivalent uninuclear promolecules and the number (b^*) of inequivalent binuclear promolecules satisfy the relation $u^* - b^* = 5 - 4 = 1$.

The examples shown in figures 3 and 8 can be generalized as follows. If a given 3D-tree is an unbalanced one, a vertex selected from each orbit of vertices and an edge selected from each orbit of edges construct a sub-3D-tree, which has u^* vertices and b^* edges. Hence, $u^* = b^* + 1$. Thus, in any unbalanced 3D-tree, the number (u^*) of inequivalent vertices is equal to one plus the number (b^*) of inequivalent edges. This is rewritten to cover uninuclear and binuclear promolecules for an unbalanced 3D-tree as the following theorem:

Theorem 3. In any unbalanced 3D-tree, the number (u^*) of relevant uninuclear promolecules relevant to it and the number (b^*) of relevant binuclear promolecules satisfy the relationship $u^* - b^* = 1$.

Let U_k be the number of unbalanced 3D-trees of carbon content k. The corresponding counting series is represented as follows:

$$U(x) = \sum_{k=1}^{\infty} U_k x^k. \tag{4}$$

Theorem 2 indicates that the contribution of the uninuclear promolecules (e.g., **40**–**42**) to the coefficient U_k should be zero per balanced 3D-tree, even though the contribution of the uninuclear promolecules (e.g., **40**–**42**) to the coefficient G_k is one or more (i.e., u^*) per balanced 3D-tree. On the other hand, theorem 3 indicates that the contribution of the uninuclear promolecules (e.g., **17**–**21**) to the coefficient U_k should be only unit per unbalanced 3D-tree, even though the contribution of the uninuclear promolecules (**17**–**21**) to the coefficient G_k is one or more (i.e., u^*) per unbalanced 3D-tree.

Theorems 2 and 3 indicates that the generating function (equation 4) is represented by

$$U(x) = G(x) - C(x), \tag{5}$$

which counts inequivalent unbalanced trees. The generating function $G(x)$ (equation 2) counts uninuclear promolecules, while the generating function $C(x)$ (equation 3) counts binuclear promolecules, which are contained as contaminants in the former set of uninuclear promolecules.

Theorem 4. Let $G(x)$ (equation 2) be a generating function for counting uninuclear promolecules. Let $C(x)$ (equation 3) be a generating function for counting binuclear promolecules. Then, the subtraction $U(x) = G(x) - C(x)$ (equation 5) gives the numbers of inequivalent balanced 3D-trees as its coefficients, where any one selected from each set of equivalent unbalanced 3D-trees is left to be counted just once. Thus, the coefficients satisfy the relationship $U_k = G_k - C_k$ (k: non-negative integers).

The expression "any one selected from each set of equivalent unbalanced 3D-trees is left to be counted just once" means that there is no criterion for selecting a specified unbalanced 3D-tree. For example, any one of **12**–**16** in figure 3 gives a single unbalanced 3D-tree (**3**) if the symbol for a nucleus • is deleted.

If the number evaluated by $G(x)$ contains irregularity due to contaminants of *meso*-type, the functional equation $C(x)$ used in equation 5 (theorem 4) should be corrected to give corrected values of $U(x)$. Such corrections will be discussed below in detail.

2.5. Cores for unbalanced 3D-trees

The second approach to discuss the congruence between such uninuclear promolecules as relevant to a single 3D-tree is based on the methodology in which the correspondence between the uninuclear promolecules and the relevant binuclear ones is determined after the selection of a specified uninuclear promolecule with a core.

2.5.1. Other modes of dichotomy

According to Jordan [30], there are two modes of dichotomy for classifying trees. The dichotomy of central/bicentral trees is based on the presence of a center or a bicenter, while the dichotomy of centroidal/bicentroidal trees is based on the presence of a centroid or a bicentroid. The two proligands attaching to a given balance-edge are congruent because of definition 1. This means that the balance-edge is identical with the edge of a bicenter as well as with the edge of a bicentroid.

Each unbalanced 3D-tree, whether it is central or bicentral (or centroidal or bicentroidal), has a special vertex, which is different from the other vertices. This means that each unbalanced 3D-tree can be treated as a central 3D-tree (or a centroidal 3D-tree). Let us call the special vertex a *core* by the following definition:

Definition 3. For any unbalanced tree, we can select a core for discussing its congruence to other 3D-trees:

1. A center of a given tree if present can be selected as a core for discussing its congruence to other 3D-trees. Similarly, a centroid of a given tree if present can be a core for discussing its congruence to other 3D-trees.
2. If a given tree has a bicenter other than a balance-edge, either one of the two terminal vertices of the bicenter can be selected as such a core as described above, because they are not equivalent. Similarly, if a given tree has a bicentroid other than a balance-edge, either one of the two terminal vertices of the bicentroid can be selected as such a core as described above, because they are not equivalent.

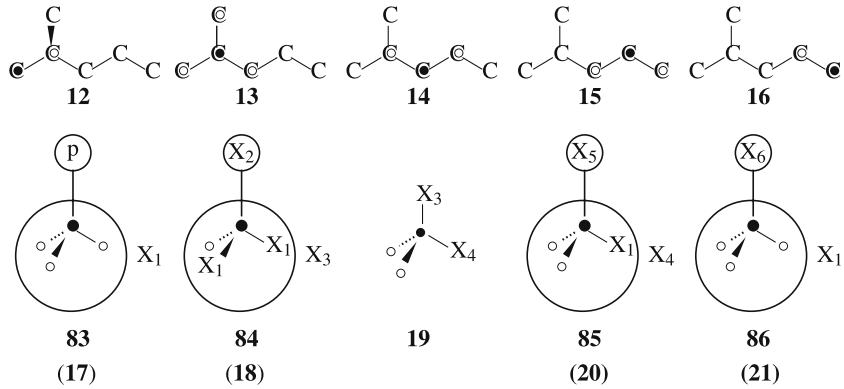

Figure 9. A representative uninuclear 3D-tree **14** (or promolecule **19**) as well as contaminants (**12**, **13**, **15**, and **16**), which are ascribed to binuclear promolecules (**83**–**86**).

To discuss the congruence of unbalanced 3D-trees, a center or either one vertex of a bicenter is here selected as a core. It should be noted that essentially equivalent discussions are available, if a centroid or either one vertex of a bicentroid is selected as a core.

For example, the center of the 3D-tree (**3**) is a vertex shown by the symbol • in the uninuclear 3D-tree (**14**). The center is selected as a core and the corresponding uninuclear 3D-tree (**14**) is selected as a representative among the corresponding uninuclear 3D-trees (**12**–**16**) shown in figure 3.

The promolecule (**19**) corresponding to **14** is considered as a representative of the uninuclear promolecules (**17**–**21**), as shown in figure 9. This means that the promolecule (**19**) is counted just once and the other promolecules (**17**, **18**, **20**, and **21**) should be left out of our calculations as contaminants. For this purpose, the contaminant promolecules (**17**, **18**, **20**, and **21**) are rewritten as binuclear promolecule **83**–**86**, as shown in figure 9.

The binuclear promolecule (**83**) corresponding to the contaminant uninuclear promolecule (**17**) is recognized to contain a proligand p and another proligand X_1, where the former proligand p retains the core selected for the representative (**14** or **19**). Once the representative (**14** or **19**) is selected, the proligand p is regarded as being fixed. On the same line, the binuclear promolecules **84**–**86** contain proligands which are considered to be fixed, i.e., X_2 for **84**, X_5 for **85**, and X_6 for **86**, as shown in figure 9.

The procedure described above results in the one-to-one correspondence between the uninuclear promolecules and the binuclear promolecules shown in figure 9, i.e., **12/83**, **13/84**, **15/85**, and **16/86**.

In general, once a representative (as a uninuclear promolecule) having a core vertex (e.g., a center) is selected for any unbalanced 3D-tree, the remaining contaminant 3D-trees (as uninuclear promolecules) are regarded as binuclear promolecules, where one proligand of each binuclear promolecule contains the

core of the representative selected. Moreover the proligand containing the core is considered to be fixed after the selection of the representative.

Combinatorial enumeration of uninuclear promolecules contains the same process as that of binuclear promolecules, if one proligand is fixed.

Theorem 5. Suppose that one proligand of a given 3D-tree is fixed. Consider the set of uninuclear promolecules which are generated by using all of planted 3D-trees as the other proligands as well as the set of binuclear promolecules which are generated by using all of planted 3D-trees as the other proligand. The two sets are identical under the condition that the first selected proligand is fixed.

This point has been discussed in terms of the relationship between proligands and ligands [16–18].

2.5.2. Deletion of contaminants

Theorem 5 indicates that the deletion of the contaminants (**12**, **13**, **15**, and **16** or equivalently **17**, **18**, **20**, and **21**) can be replaced by the deletion of the binuclear promolecules (**83**–**86**). Thereby, there remains the representative **14** or **19**. It follows that the generating function $U(x) = G(x) - C(x)$ can be used to evaluate the number of such representatives (i.e., the number of inequivalent unbalanced 3D-trees). Note that the generating function $G(x)$ (equation 2) counts uninuclear promolecules, while the generating function $C(x)$ (equation 3) counts binuclear promolecules as contaminants. This conclusion is the same as equation 5.

Next, we shall examine balanced trees. For example, figure 6 shows the relationship between the balance-edge of the balanced 3D-tree (**32**) and the nucleus (•) of each uninuclear 3D-trees **37**–**39** (or equivalently each uninuclear promolecule **40**–**42**).

The binuclear 3D-tree **46** (or equivalently the binuclear promolecule **43**) which corresponds to the uninuclear 3D-tree **37** (or equivalently the uninuclear promolecule **40**) is rewritten as **87**, which contain proligands p and X_1 (figure 10). Because the proligand p involves the balance-edge, the p is considered to be fixed. On the same line, the proligand X_2 contained in **88** is considered to be fixed.

According to theorem 5, the counting as uninuclear 3D-trees (e.g., **37** and **38**) gives the same results as the counting as binuclear 3D-trees (e.g., **87** and **88**).

On the other hand, the nucleus (•) of the uninuclear 3D-tree **39** (or equivalently each uninuclear promolecule **42**) produces no proligand containing the balanced edge. As shown in the rewritten promolecule **89**, the proligand X_4 does not contain the balance-edge but contains the either terminal vertex of the balance-edge. Even in this case, the counting as uninuclear 3D-trees (e.g., **39**) gives the same results as the counting as binuclear 3D-trees (e.g., **89**) according to theorem 5.

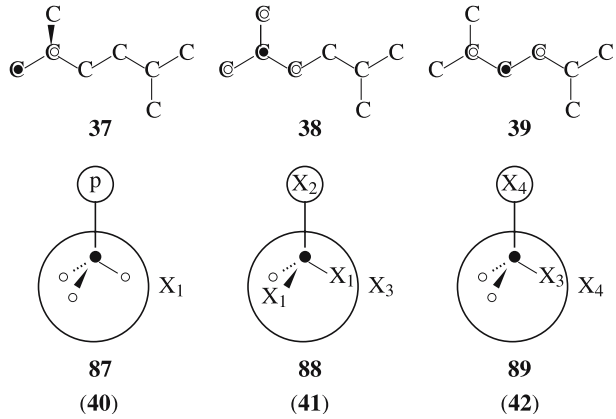

Figure 10. Uninuclear 3D-trees **37**–**39** for a balanced tree. They are ascribed to binuclear promolecules (**87**–**89**).

It follows that the generating function $G(x) - C(x)$ for balanced 3D-trees vanishes so as to exhibit no contribution to the number of inequivalent unbalanced 3D-trees. This conclusion is the same as equation 5, which also shows no contribution of balanced 3D-trees.

The discussions described in this subsection provide us with an alternative proof of equation 5. For the sake of further discussions, the conclusion of the second proof is summarized as a theorem:

Theorem 6. Let $G(x)$ (equation 2) be a generating function for counting uninuclear promolecules. Let $C(x)$ (equation 3) be a generating function for counting binuclear promolecules. Then, the subtraction $U(x)=G(x) - C(x)$ (equation 5) gives the numbers of inequivalent balanced 3D-trees as its coefficients, where each of the inequivalent unbalanced 3D-trees is characterized by a core. Thus, the coefficients satisfy the relationship $U_k = G_k - C_k$ (k: non-negative integers).

Compare theorem 6 with theorem 4. The expression "each of the inequivalent unbalanced 3D-trees is characterized by a core" means that the selected core is a criterion for selecting a specified unbalanced 3D-tree. For example, **14** selected among **12**–**16** (figure 3) gives a single unbalanced 3D-tree (**3**), where the core • is specified so as to leave **14** (or **19**).

If the number evaluated by $G(x)$ contains irregularity due to contaminants of *meso*-type, the functional equation $C(x)$ used in equation 5 (theorem 6) should be corrected to give corrected values of $U(x)$ on the same line as theorem 4.

3. Combinatorial enumeration of 3D-trees

3.1. Ligand inventories of three kinds

According to Fujita's proligand method [16–18], promolecules as stereoisomers can be counted by placing proligands on a given skeleton, where the modes of substitution are controlled by three kinds of sphericities of cycles. The sphericity of each cycle determines the chirality fittingness for accommodating achiral and/or chiral proligands, which is represented by a generating function. A homospheric d-cycle is characterized by a sphericity index a_d, which is replaced by $a(x^d)$ to generate a ligand inventory. The resulting ligand inventory $a(x)$ is a generating function for enumerating achiral proligands. An enantiospheric d-cycle is characterized by a sphericity index c_d, which is replaced by $c(x^d)$ to generate a ligand inventory. The resulting ligand inventory $c(x)$ is a generating function for enumerating ordered enantiomeric pairs called "diploids", where we use $c(x^2)$ because d is even. A hemispheric d-cycle is characterized by a sphericity index b_d, which is replaced by $b(x^d)$ to generate a ligand inventory. The resulting ligand inventory $b(x)$ is a generating function for enumerating achiral proligands and chiral proligands, where two enantiomers of each pair counted separately. Hence, we presume the following generating functions:

$$a(x) = \sum_{k=0}^{\infty} \alpha_k x^k, \tag{6}$$

$$c(x^2) = \sum_{k=0}^{\infty} \gamma_{2k} x^{2k}, \tag{7}$$

$$b(x) = \sum_{k=0}^{\infty} \beta_k x^k, \tag{8}$$

where we place $\alpha_0 = 1$, $\gamma_0 = 1$, $\beta_0 = 1$ for the trivial cases; and α_k, γ_k, and β_k represent the numbers of proligands at issue.

For the purpose of enumerating 3D-trees of degree 4 (or alkanes), planted 3D-trees enumerated under the point group $\mathbf{C}_{3v}$ are used as proligands on the basis of Fujita's proligand method [16–18]. Thereby, the following functional equations for evaluating α_k, γ_k, and β_k obtained:

$$a(x) = 1 + xa(x)c(x^2), \tag{9}$$

$$c(x^2) = 1 + \frac{x^2}{3}\left(c(x^2)^3 + 2c(x^6)\right), \tag{10}$$

$$b(x) = 1 + \frac{x}{3}\left(b(x)^3 + 2b(x^3)\right), \tag{11}$$

although the derivation of these equations for enumerating such proligands (planted 3D-trees) will be mentioned elsewhere. The values of α_k, γ_k, and β_k are recursively calculated by using equations 9–11. In order to enumerate 3D-trees, the results up to carbon content 20 are shown as the following ligand-counting series:

$$\begin{aligned} a(x) = {} & 1 + x + x^2 + 2x^3 + 3x^4 + 5x^5 + 8x^6 + 14x^7 + 23x^8 \\ & + 41x^9 + 69x^{10} + 122x^{11} + 208x^{12} + 370x^{13} \\ & + 636x^{14} + 1134x^{15} + 1963x^{16} + 3505x^{17} \\ & + 6099x^{18} + 10908x^{19} + 19059x^{20} + \cdots, \end{aligned} \tag{12}$$

$$\begin{aligned} c(x^2) = {} & 1 + x^2 + x^4 + 2x^6 + 5x^8 + 11x^{10} + 28x^{12} \\ & + 74x^{14} + 199x^{16} + 551x^{18} + 1553x^{20} + 4436x^{22} + 12832x^{24} \\ & + 37496x^{26} + 110500x^{28} + 328092x^{30} + 980491x^{32} + 2946889x^{34} \\ & + 8901891x^36 + 27012286x^{38} + 82300275x^{40} + \cdots, \end{aligned} \tag{13}$$

$$\begin{aligned} b(x) = {} & 1 + x + x^2 + 2x^3 + 5x^4 + 11x^5 + 28x^6 + 74x^7 \\ & + 199x^8 + 551x^9 + 1553x^{10} + 4436x^{11} + 12832x^{12} \\ & + 37496x^{13} + 110500x^{14} + 328092x^{15} + 980491x^{16} \\ & + 2946889x^{17} + 8901891x^{18} + 27012286x^{19} + 82300275x^{20} + \cdots, \end{aligned} \tag{14}$$

where each coefficient gives the value α_k, γ_k, or β_k for the generating function shown in equations. 6–8. It should be noted that the coefficient α_k of equation 12 indicates the number of achiral mono-substituted alkanes of carbon content k; that the coefficient γ_k of equation 13 indicates the number of achiral mono-substituted alkanes plus enantiomeric pairs of chiral mono-substituted alkanes both of carbon content k (i.e., so-called "diploids"); that the coefficient β_k of equation 14 indicates the number of achiral and chiral mono-substituted alkanes of carbon content k, which are counted separately. The numbers of such mono-substituted alkanes as enumerated in terms of the sphericities of three categories can be regarded as the numbers of alkyl ligands, which are necessary to enumerate alkanes as stereoisomers. At the same time, they can be regarded as the numbers of planted 3D-trees, which are necessary to enumerate 3D-trees.

3.2. Enumeration of unbalanced 3D-trees

In the preceding discussion on $G(x)$, $C(x)$, and $U(x)$, the automorphism groups for uninuclear and binuclear promolecules are not specified. Here, combinatorial enumerations are conducted under the four conditions, which are denoted by the following superscripts. The automorphism groups are determined according to these conditions.

1. The symbol (AC) is concerned with the number of inequivalent 3D-trees, where achiral ones (A) plus enantiomeric pairs (C) of chiral ones are

counted. Note that each enantiomeric pair is counted just once, though the pair is composed of two enantiomers. As for a tetrahedral skeleton for enumerating uninuclear promolecules, the $\mathbf{T}_d$ group is used as the automorphism group. The $\mathbf{D}_{\infty h}$ or its factor group $\mathbf{D}_{\infty h}/\mathbf{C}_{\infty}$ is used to evaluate the number of binuclear promolecules.

2. The symbol (AC^2) is concerned with the number of inequivalent 3D-trees which are achiral (A) and chiral (C^2), where the two chiral 3D-trees of each enantiomeric pair are counted separately. For this purpose, the $\mathbf{T}$ group and the $\mathbf{D}_{\infty}$ (or its factor group $\mathbf{D}_{\infty}/\mathbf{C}_{\infty}$) are used.
3. The symbol (A) is concerned with the number of inequivalent 3D-trees which are achiral (A). For this purpose, the improper rotations of the $\mathbf{T}_d$ group and those of the $\mathbf{D}_{\infty h}$ (or its factor group $\mathbf{D}_{\infty h}/\mathbf{C}_{\infty}$) are used.
4. The symbol (C) is concerned with the number of inequivalent 3D-trees which are chiral (C). For this purpose, the $\mathbf{T}_d$ group and the $\mathbf{D}_{\infty h}$ (or its factor group $\mathbf{D}_{\infty h}/\mathbf{C}_{\infty}$) are used after modification.

3.2.1. Binuclear 3D-trees as contaminants

The first task is to evaluate the number of binuclear promolecules or 3D-trees for $C(x)$ (equation 5). As found in the preceding discussions, binuclear promolecules represent contaminants for enumerating unbalanced 3D-trees (cf. theorem 6) as well as balanced trees. Such binuclear promolecules contain a two-nodal skeleton (**31**) of $\mathbf{D}_{\infty h}$-symmetry. In order to avoid the infinite nature of the $\mathbf{D}_{\infty h}$-point group, we use the corresponding factor group of order 4:

$$\mathbf{K} = \mathbf{D}_{\infty h}/\mathbf{C}_{\infty} = \{\mathbf{C}_{\infty}I, \mathbf{C}_{\infty}C_2, \mathbf{C}_{\infty}\sigma_v, \mathbf{C}_{\infty}\sigma_h\} \tag{15}$$

and its subgroups:

$$\mathbf{K}_1 = \mathbf{C}_{\infty}/\mathbf{C}_{\infty} = \{\mathbf{C}_{\infty}I\}, \tag{16}$$

$$\mathbf{K}_2 = \mathbf{D}_{\infty}/\mathbf{C}_{\infty} = \{\mathbf{C}_{\infty}I, \mathbf{C}_{\infty}C_2\}, \tag{17}$$

$$\mathbf{K}_3 = \mathbf{C}_{\infty v}/\mathbf{C}_{\infty} = \{\mathbf{C}_{\infty}I, \mathbf{C}_{\infty}\sigma_v\}, \tag{18}$$

$$\mathbf{K}_4 = \mathbf{C}_{\infty h}/\mathbf{C}_{\infty} = \{\mathbf{C}_{\infty}I, \mathbf{C}_{\infty}\sigma_h\}, \tag{19}$$

$$\mathbf{K}_5 = \mathbf{K} = \mathbf{D}_{\infty h}/\mathbf{C}_{\infty}, \tag{20}$$

according to the treatment reported previously [21]. Thereby, the two positions of the skeleton, which are governed by the right coset representation $(\mathbf{C}_{\infty v}\backslash)\mathbf{D}_{\infty h}$, are in turn considered to be governed by the right coset representation of the factor group, i.e., $(\mathbf{K}_3\backslash)\mathbf{K}$. In particular, the factor group $\mathbf{K}$ is isomorphic to the point group $\mathbf{C}_{2v} = \{I, C_2, \sigma_{v(1)}, \sigma_{v(2)}\}$, while the subgroup $\mathbf{K}_3$ is isomorphic to the point group $\mathbf{C}_s = \{I, \sigma_{v(1)}\}$, where we place $\sigma_{v(1)} = \sigma_v$ and $\sigma_{v(2)} = \sigma_h$. Geometrically speaking, the infinite number of dihedral C_2-axes of the two-nodal skeleton is reduced into a single C_2-axis; the infinite number of mirror planes σ_v is reduced into a single $\sigma_{v(1)}$; and the horizontal mirror plane

σ_h is changed into a single $\sigma_{v(2)}$. This means that the sphericity indices for the RCR $(\mathbf{C}_{\infty v}\backslash)\mathbf{D}_{\infty h}$ having infinite symmetry operations can be discussed through the RCR $(\mathbf{K}_3\backslash)\mathbf{K}$ having finite operations on the analogy of the RCR $(\mathbf{C}_s\backslash)\mathbf{C}_{2v}$.

When we sequentially number the two substitution positions of the two-nodal skeleton for the binuclear 3D-trees, we can obtain the following right coset representation:

$$(\mathbf{K}_3\backslash)\mathbf{K} = \{(1)(2),\ (1\ 2),\ \overline{(1)(2)},\ \overline{(1\ 2)}\}, \tag{21}$$

which permutes the two positions, where each overbar represents the alternation of the chirality of a proligand occupying the position. The products of sphericity indices b_1^2 and b_2 are assigned to the cycles (1)(2) and (1)(2), while a_1^2 and c_2 are assigned to $\overline{(1)(2)}$ and $\overline{(1\ 2)}$. Following theorem 1 of [18], the CI-CF for this case is obtained as follows:

$$\text{CI-CF}(\mathbf{K}; \$_d) = \frac{1}{4}\left(b_1^2 + b_2 + a_1^2 + c_2\right), \tag{22}$$

where the symbol $\$_d$ represents a sphericity index, a_d, c_d, or b_d, according to the respective sphericity. An equation equivalent to equation 22 has been reported previously on the basis of Fujita's USCI approach [21].

Let $C_k^{(AC)}$ be the number of binuclear 3D-trees of carbon content k, which are achiral ones plus enantiomeric pairs of chiral ones. They are enumerated by using the automorphism group $\mathbf{K}(= \mathbf{D}_{\infty h}/\mathbf{C}_\infty)$.

$$C(x)^{(AC)} = \sum_{k=1}^{\infty} C_k^{(AC)} x^k. \tag{23}$$

The sphericity indices, a_d, c_d, and b_d, are replaced by $a(x^d) - 1$, $c(x^d) - 1$, and $b(x^d) - 1$, respectively. Note that the coefficient of the term $x^0(=1)$ in equation 12, 13, or 14 is unnecessary to the use for binuclear promolecules. Thereby, equation 22 is converted into the corresponding counting series as follows:

$$C(x)^{(AC)} = \frac{1}{4}\left\{(b(x) - 1)^2 + (b(x^2) - 1) + (a(x) - 1)^2 + (c(x^2) - 1)\right\}. \tag{24}$$

The ligand inventories shown in equations 12–14 are introduced into equation 24 and the resulting equation is expanded to give the following generating function:

$$\begin{aligned} C(x)^{(AC)} = {} & x^2 + x^3 + 3x^4 + 6x^5 + 15x^6 + 34x^7 + 89x^8 + 226x^9 + 619x^{10} \\ & + 1709x^{11} + 4882x^{12} + 14104x^{13} + 41463x^{14} + 122930x^{15} \\ & + 367966x^{16} + 1108199x^{17} + 3357386x^{18} + 10217632x^{19} \\ & + 31225699x^{20} + \cdots, \end{aligned} \tag{25}$$

where the coefficient $C_k^{(AC)}$ of the term x^k represents the number of inequivalent binuclear promolecules, which are recognized as contaminants.

Theorem 3 of Ref. 18 for the enumeration of ligands under the action of the maximum chiral subgroup can be applied to this case so as to derive the following CI-CF:

$$\text{CI-CF}(\mathbf{K}_2; b_d) = \frac{1}{2}\left(b_1^2 + b_2\right), \tag{26}$$

which counts achiral promolecules and chiral promolecules, where two enantiomers of each pair are counted separately.

Let $\widehat{C}_k^{(AC^2)}$ be the uncorrected number of binuclear 3D-trees of carbon content k, which are achiral and chiral.

$$\widehat{C}(x)^{(AC^2)} = \sum_{k=1}^{\infty} \widehat{C}_k^{(AC^2)} x^k. \tag{27}$$

By replacing b_d by $b(x^d) - 1$, equation 26 is converted into the corresponding functional equation as follows:

$$\widehat{C}(x)^{(AC^2)} = \frac{1}{2}\left\{(b(x) - 1)^2 + (b(x^2) - 1)\right\}. \tag{28}$$

The ligand inventories shown in equations 12–14 are introduced into equation 28 and the resulting equation is expanded to give the following generating function:

$$\begin{aligned}\widehat{C}(x)^{(AC^2)} = {} & x^2 + x^3 + 3x^4 + 7x^5 + 19x^6 + 49x^7 + 139x^8 + 384x^9 + 1104x^{10} \\ & + 3180x^{11} + 9306x^{12} + 27390x^{13} + 81373x^{14} + 243077x^{15} \\ & + 730698x^{16} + 2206994x^{17} + 6697203x^{18} + 20403645x^{19} \\ & + 62392611x^{20} + \cdots .\end{aligned} \tag{29}$$

The first proposition of theorem 4 for the enumeration of achiral ligands [18] can be applied to this case so as to derive the following CI-CF$_A$:

$$\begin{aligned}\text{CI-CF}_A(\mathbf{K}, \$_d) &= 2\text{CI-CF}(\mathbf{K}, \$_d) - \text{CI-CF}(\mathbf{K}_2, b_d) \\ &= \frac{1}{2}\left(a_1^2 + c_2\right),\end{aligned} \tag{30}$$

which counts achiral promolecules only, where each pair of enantiomers is counted just once.

Let $\widehat{C}_k^{(A)}$ be the uncorrected number of binuclear 3D-trees of carbon content k, which are achiral.

$$\widehat{C}(x)^{(A)} = \sum_{k=1}^{\infty} \widehat{C}_k^{(A)} x^k. \tag{31}$$

By replacing a_d, c_d, and b_d by $a(x^d) - 1$, $c(x^d) - 1$, and $b(x^d) - 1$, respectively, equation 30 is converted into the corresponding functional equation as follows:

$$\widehat{C}(x)^{(A)} = \frac{1}{2}\left\{(a(x) - 1)^2 + (c(x^2) - 1)\right\}. \tag{32}$$

The ligand inventories shown in equations 12–14 are introduced into equation 32 and the resulting equation is expanded to give the following generating function:

$$\begin{aligned}\widehat{C}(x)^{(A)} = {} & x^2 + x^3 + 3x^4 + 5x^5 + 11x^6 + 19x^7 + 39x^8 + 68x^9 + 134x^{10} \\ & + 238x^{11} + 458x^{12} + 818x^{13} + 1553x^{14} + 2783x^{15} + 5234x^{16} \\ & + 9404x^{17} + 17569x^{18} + 31619x^{19} + 58787x^{20} + \cdots .\end{aligned} \tag{33}$$

It should be noted that the enumeration results shown in equation 33 contain the participation of balanced binuclear 3D-trees of *meso*-type (e.g., p$\overline{\text{p}}$), which are unnecessary to be counted as contaminants. However, this unnecessary participation is deleted by adding the number of balanced binuclear 3D-trees, as described later.

In order to avoid the unnecessary participation of the *meso*-type, the term c_2 for treating *meso*-type in equation 30 is replaced by the term a_2. Thereby, we obtain the following equation:

$$\frac{1}{2}\left(a_1^2 + a_2\right). \tag{34}$$

Let $C_k^{(A)}$ be the (corrected) number of inequivalent binuclear 3D-trees of carbon content k, which are achiral but not *meso*-type.

$$C(x)^{(A)} = \sum_{k=1}^{\infty} C_k^{(A)} x^k. \tag{35}$$

By replacing a_d by $a(x^d) - 1$, equation 34 is converted into the corresponding functional equation as follows:

$$C(x)^{(A)} = \frac{1}{2}\left\{(a(x) - 1)^2 + (a(x^2) - 1)\right\}. \tag{36}$$

The ligand inventories shown in equations 12–14 are introduced into equation 36. The resulting equation is expanded to give the following generating function:

$$\begin{aligned}C(x)^{(A)} = {} & x^2 + x^3 + 3x^4 + 5x^5 + 11x^6 + 19x^7 + 38x^8 + 68x^9 + 131x^{10} \\ & + 238x^{11} + 448x^{12} + 818x^{13} + 1523x^{14} + 2783x^{15} + 5146x^{16} \\ & + 9404x^{17} + 17314x^{18} + 31619x^{19} + 58045x^{20} + \cdots .\end{aligned} \tag{37}$$

The second proposition of theorem 4 for the enumeration of chiral ligands [18] can be applied to obtain the following CI-CF$_C$:

$$\begin{aligned}\text{CI-CF}_C(\mathbf{K}, \$_d) &= \text{CI-CF}(\mathbf{K}_2, b_d) - \text{CI-CF}(\mathbf{K}, \$_d) \\ &= \frac{1}{4}\left(b_1^2 + b_2 - a_1^2 - c_2\right), \end{aligned} \tag{38}$$

which counts chiral promolecules only. As found easily, equation 38 is obtained by subtracting equation 30 from equation 22.

Let $\widehat{C}_k^{(C)}$ be the uncorrected number of binuclear 3D-trees of carbon content k, which are enantiomeric pairs of chiral ones.

$$\widehat{C}(x)^{(C)} = \sum_{k=1}^{\infty} \widehat{C}_k^{(C)} x^k. \tag{39}$$

By replacing a_d, c_d, and b_d by $a(x^d) - 1$, $c(x^d) - 1$, and $b(x^d) - 1$, respectively, equation 38 is converted into the corresponding functional equation as follows:

$$\widehat{C}(x)^{(C)} = \frac{1}{4}\left\{(b(x) - 1)^2 + (b(x^2) - 1) - (a(x) - 1)^2 - (c(x^2) - 1)\right\}. \tag{40}$$

The ligand inventories shown in equations 12–14 are introduced into equation 40 and the resulting equation is expanded to give the following generating function:

$$\begin{aligned}\widehat{C}(x)^{(C)} = {} & x^5 + 4x^6 + 15x^7 + 50x^8 + 158x^9 + 485x^{10} \\ & + 1471x^{11} + 4424x^{12} + 13286x^{13} + 39910x^{14} + 120147x^{15} + 362732x^{16} \\ & + 1098795x^{17} + 3339817x^{18} + 10186013x^{19} + 31166912x^{20} + \cdots. \end{aligned} \tag{41}$$

On the same line as equation 38 is obtained by subtracting equations 30 from 22, the subtraction of equations 34 from 22 gives the following equation:

$$\frac{1}{4}\left(b_1^2 + b_2 - a_1^2 + c_2 - 2a_2\right), \tag{42}$$

which is related to equation 34 without the participation of *meso*-type.

Let $C_k^{(C)}$ be the (corrected) number of binuclear 3D-trees of carbon content k, which are enantiomeric pairs of chiral ones.

$$C(x)^{(C)} = \sum_{k=1}^{\infty} C_k^{(C)} x^k, \tag{43}$$

where the participation of *meso*-type is avoided according to equation 34. By replacing a_d, c_d, and b_d by $a(x^d)-1$, $c(x^d)-1$, and $b(x^d)-1$, respectively, equation 42 is converted into the corresponding functional equation as follows:

$$C(x)^{(C)} = \frac{1}{4}\left\{(b(x)-1)^2 + (b(x^2)-1) - (a(x)-1)^2 + (c(x^2)-1) - 2(a(x^2)-1)\right\}. \quad (44)$$

The ligand inventories shown in equations 12–14 are introduced into equation 44 and the resulting equation is expanded to give the following generating function:

$$C(x)^{(C)} = x^5 + 4x^6 + 15x^7 + 51x^8 + 158x^9 + 488x^{10} + 1471x^{11} + 4434x^{12} + 13286x^{13} + 39940x^{14} + 120147x^{15} + 362820x^{16} + 1098795x^{17} + 3340072x^{18} + 10186013x^{19} + 31167654x^{20} + \cdots. \quad (45)$$

To introduce the correction by equation 42 into the evaluation by $\widehat{C}(x)^{(AC^2)}$, we sum up equations 22 and 42 as follows:

$$\frac{1}{4}\left(b_1^2 + b_2 + a_1^2 + c_2\right) + \frac{1}{4}\left(b_1^2 + b_2 - a_1^2 + c_2 - 2a_2\right) = \frac{1}{2}\left(b_1^2 + b_2\right) + \frac{1}{2}\left(c_2 - a_2\right). \quad (46)$$

Let $C_k^{(AC^2)}$ be the (corrected) number of binuclear 3D-trees of carbon content k, which are achiral and chiral:

$$C(x)^{(AC^2)} = \sum_{k=1}^{\infty} C_k^{(AC^2)} x^k. \quad (47)$$

By replacing a_d, c_d, and b_d by $a(x^d)-1$, $c(x^d)-1$, and $b(x^d)-1$, respectively, equation 46 is converted into the corresponding functional equation as follows:

$$C(x)^{(AC^2)} = \frac{1}{2}\left\{(b(x)-1)^2 + (b(x^2)-1)\right\} + \frac{1}{2}\left\{(c(x^2)-1) - (a(x^2)-1)\right\}. \quad (48)$$

Compare this equation with equation 28. The terms within the last pair of braces in equation 48 indicate the correction at issue.

The ligand inventories shown in equations 12–14 are introduced into equation 48 and the resulting equation is expanded to give the following generating function:

$$C(x)^{(AC^2)} = x^2 + x^3 + 3x^4 + 7x^5 + 19x^6 + 49x^7 + 140x^8 + 384x^9 + 1107x^{10} + 3180x^{11} + 9316x^{12} + 27390x^{13} + 81403x^{14} + 243077x^{15} + 730786x^{16} + 2206994x^{17} + 6697458x^{18} + 20403645x^{19} + 62393353x^{20} + \cdots \quad (49)$$

The corrected and uncorrected equations for evaluating contaminants satisfy the following equations:

$$C(x)^{(AC)} = C(x)^{(A)} + C(x)^{(C)}, \tag{50}$$

$$C(x)^{(AC)} = \widehat{C}(x)^{(A)} + \widehat{C}(x)^{(C)}, \tag{51}$$

$$C(x)^{(AC^2)} = C(x)^{(AC)} + C(x)^{(C)}, \tag{52}$$

$$\widehat{C}(x)^{(AC^2)} = C(x)^{(AC)} + \widehat{C}(x)^{(C)}. \tag{53}$$

Thus, equation 50 is derived from equations 24, 36, and 44 or alternatively from equations 25, 37, and 45; and equation 51 is derived from equations 24, 32, and 40 or alternatively from equations 25, 33, and 41. In addition, equation 52 is derived from equations 48, 24, and 44 or alternatively from equations 49, 25, and 45; and equation 53 is derived from equations 28, 24, and 40 or alternatively from equations 29, 25, and 41.

3.2.2. Uninuclear 3D-trees for evaluating gross numbers

The next task is to evaluate the number of uninuclear 3D-trees for $G(x)$ (equation 5). The uninuclear skeleton (**30**) belongs to $\mathbf{T}_d$-symmetry so that the four substitution positions are governed by the right coset representation (RCR) $(\mathbf{C}_{3v}\backslash)\mathbf{T}_d$ according to the USCI approach [23] and the proligand method [16–18]. By applying theorem 1 of Ref. 18 to this case, the CI-CF is calculated as follows:

$$\text{CI-CF}(\mathbf{T}_d, \$_d) = \frac{1}{24}(b_1^4 + 3b_2^2 + 8b_1b_3 + 6a_1^2c_2 + 6c_4), \tag{54}$$

which counts achiral promolecules and enantiomeric pairs of chiral promolecules. Note that each pair of enantiomers is counted just once in this enumeration.

Let $G_k^{(AC)}$ be the number of achiral uninuclear promolecules plus enantiomeric pairs of chiral uninuclear promolecules of carbon content k. Then, a generating function for enumerating them can be written as follows:

$$G(x)^{(AC)} = \sum_{k=1}^{\infty} G_k^{(AC)} x^k. \tag{55}$$

By replacing a_d, c_d, and b_d by $a(x^d)$, $c(x^d)$, and $b(x^d)$, respectively, equation 54 is converted into the corresponding counting series as follows:

$$G(x)^{(AC)} = \frac{x}{24}\big(b(x)^4 + 3b(x^2)^2 + 8b(x)b(x^3) + 6a(x)^2c(x^2) + 6c(x^4)\big). \tag{56}$$

where the multiplication by x is necessary because equation 54 for $\text{CI-CF}(\mathbf{T}_d, \$_d)$ ignores the nucleus of the parent promolecule tentatively (cf. **30**). Note that the

term for a null vertex (i.e., $x^0 = 1$) should be taken into consideration in the derivation of equation 56.

The ligand inventories shown in equations 12–14 are introduced into equation 56 and the resulting equation is expanded to give the following generating function:

$$\begin{aligned} G(x)^{(AC)} = {} & x + x^2 + 2x^3 + 4x^4 + 9x^5 + 18x^6 + 43x^7 + 103x^8 + 264x^9 + 696x^{10} \\ & + 1912x^{11} + 5363x^{12} + 15403x^{13} + 44848x^{14} + 132277x^{15} + 393657x^{16} \\ & + 1180704x^{17} + 3562712x^{18} + 10807244x^{19} + 32927721x^{20} + \cdots . \end{aligned} \tag{57}$$

Theorem 3 of Ref. 18 for the enumeration of ligands under the action of the maximum chiral subgroup can be applied to the derivation of the CI-CF for enumeration based on the **T**:

$$\text{CI-CF}(\mathbf{T}, b_d) = \frac{1}{12}\left(b_1^4 + 3b_2^2 + 8b_1 b_3\right), \tag{58}$$

which counts achiral promolecules and chiral promolecules, where two enantiomers of each pair are counted separately.

Let $G_k^{(AC^2)}$ be the number of achiral promolecules plus chiral promolecules of carbon content k, where two enantiomers of each pair are counted separately. Then, a generating function for enumerating them is obtained as follows:

$$G(x)^{(AC^2)} = \sum_{k=0}^{\infty} G_k^{(AC^2)} x^k. \tag{59}$$

Because equation 58 for CI-CF($\mathbf{T}, b_d$) ignores the core of the parent promolecule tentatively (cf., **30**), the following functional equation is obtained by multiplying by x:

$$G(x)^{(AC^2)} = \frac{x}{12}\left(b(x)^4 + 3b(x^2)^2 + 8b(x)b(x^3)\right), \tag{60}$$

after replacing b_d of equation 58 by $b(x^d)$. The ligand inventory shown in equation 14 is introduced into equation 60 so as to obtain the target number as the coefficient $G_k^{(AC^2)}$ of the term x^k of equation 61:

$$\begin{aligned} G(x)^{(AC^2)} = {} & x + x^2 + 2x^3 + 4x^4 + 10x^5 + 22x^6 + 60x^7 + 158x^8 + 439x^9 + 1229x^{10} \\ & + 3525x^{11} + 10178x^{12} + 29802x^{13} + 87862x^{14} + 261204x^{15} \\ & + 781198x^{16} + 2350249x^{17} + 7105081x^{18} \\ & + 21577415x^{19} + 65787902x^{20} + \cdots \end{aligned} \tag{61}$$

The first proposition of theorem 4 for the enumeration of achiral ligands [18] can be applied to the present case so as to derive the following CI-CF$_A$:

$$\begin{aligned}\text{CI-CF}_A(\mathbf{T}_d, \$_d) &= 2\text{CI-CF}(\mathbf{T}_d, \$_d) - \text{CI-CF}(\mathbf{T}, b_d) \\ &= \frac{1}{2}(a_1^2 c_2 + c_4),\end{aligned} \tag{62}$$

which counts achiral promolecules only.

Let $G_k^{(A)}$ be the number of achiral promolecules of carbon content k, which appears as each coefficient of the following generating function:

$$G(x)^{(A)} = \sum_{k=0}^{\infty} G_k^{(A)} x^k. \tag{63}$$

By replacing a_d, c_d, and b_d by $a(x^d)$, $c(x^d)$, and $b(x^d)$, respectively, equation 54 is converted into the corresponding functional equation as follows:

$$G(x)^{(A)} = \frac{x}{2}\big(a(x)^2 c(x^2) + c(x^4)\big). \tag{64}$$

Because equation 63 for CI-CF$_A(\mathbf{T}_d, \$_d)$ ignores the nucleus of the parent promolecule tentatively (cf. **30**), the functional equation (equation 64) is obtained by multiplying by x. The ligand inventories shown in equations 12 and 13 are introduced into equation 64 so as to obtain the target number as the coefficient $G_k^{(A)}$ of the term x^k of equation 65:

$$\begin{aligned}G(x)^{(A)} = {} & x + x^2 + 2x^3 + 4x^4 + 8x^5 + 14x^6 + 26x^7 + 48x^8 + 89x^9 + 163x^{10} \\ & + 299x^{11} + 548x^{12} + 1004x^{13} + 1834x^{14} + 3350x^{15} + 6116x^{16} \\ & + 11159x^{17} + 20343x^{18} + 37073x^{19} + 67540x^{20} + \cdots .\end{aligned} \tag{65}$$

The second proposition of theorem 4 for the enumeration of chiral ligands [18] can be applied to obtain the following CI-CF$_C$:

$$\begin{aligned}&\text{CI-CF}_C(\mathbf{T}_d, \$_d) \\ &= \text{CI-CF}(\mathbf{T}, b_d) - \text{CI-CF}(\mathbf{T}_d, \$_d) \\ &= \frac{1}{24}\left(b_1^4 + 3b_2^2 + 8b_1 b_3 - 6a_1^2 c_2 - 6c_4\right),\end{aligned} \tag{66}$$

which counts chiral promolecules only, where each pair of enantiomers is counted just once.

Let $G_k^{(C)}$ be the number of chiral centroidal promolecules, where each pair of two enantiomers is counted just once. The corresponding generating function for enumerating them is represented as follows:

$$G(x)^{(C)} = \sum_{k=0}^{\infty} G_k^{(C)} x^k. \tag{67}$$

By replacing a_d, c_d, and b_d by $a(x^d)$, $c(x^d)$, and $b(x^d)$, respectively, after multiplying by x, equation 66 is converted into the corresponding counting series as follows:

$$G(x)^{(C)} = \frac{x}{24}\left(b(x)^4 + 3b(x^2)^2 + 8b(x)b(x^3) - 6a(x)^2c(x^2) - 6c(x^4)\right). \quad (68)$$

The same ligand inventories shown in equations 12–14 are introduced into equation 68 so as to obtain the target number as the coefficient $G_k^{(C)}$ of the term x^k of equation 69:

$$\begin{aligned} G(x)^{(C)} = {} & x^5 + 4x^6 + 17x^7 + 55x^8 + 175x^9 + 533x^{10} \\ & + 1613x^{11} + 4815x^{12} + 14399x^{13} + 43014x^{14} + 128927x^{15} + 387541x^{16} \\ & + 1169545x^{17} + 3542369x^{18} + 10770171x^{19} + 32860181x^{20} + \cdots \end{aligned} \quad (69)$$

3.2.3. Unbalanced 3D-trees

Let $U_k^{(AC)}$ be the number of inequivalent achiral unbalanced promolecules (or 3D-trees) plus inequivalent enantiomeric pairs of chiral unbalanced promolecules (or 3D-trees) of carbon content k. Then, a generating function for enumerating them can be written as follows:

$$U(x)^{(AC)} = \sum_{k=1}^{\infty} U_k^{(AC)} x^k. \quad (70)$$

The generating function is obtained by applying equation 5 to this case, i.e.,

$$U(x)^{(AC)} = G(x)^{(AC)} - C(x)^{(AC)}. \quad (71)$$

Thus, from equations 24 and equation 56, we obtain the following functional equation:

$$\begin{aligned} U(x)^{(AC)} = {} & \frac{x}{24}\left\{b(x)^4 + 3b(x^2)^2 + 8b(x)b(x^3) + 6a(x)^2c(x^2) + 6c(x^4)\right\} \\ & - \frac{1}{4}\left\{(b(x)-1)^2 + (b(x^2)-1) + (a(x)-1)^2 + (c(x^2)-1)\right\}, \end{aligned} \quad (72)$$

The ligand inventories shown in equations 12–14 are introduced into equation 72. The resulting equation is expanded to give a generating function, in which the coefficient of the term x^k is the value of $U_k^{(AC)}$. The values up to carbon content 20 are shown in the corresponding column of table 1.

Let $\widehat{U}_k^{(AC^2)}$ be the uncorrected number of inequivalent achiral unbalanced promolecules (or 3D-trees) plus inequivalent chiral unbalanced promolecules (or 3D-trees) of carbon content k, where two enantiomers of each pair are counted

Table 1
The numbers of unbalanced 3D-trees or alkanes[a].

k	$U_k^{(AC)}$	$U_k^{(AC^2)}$	$U_k^{(A)}$	$U_k^{(C)}$
1	1	1	1	0
2	0	0	0	0
3	1	1	1	0
4	1	1	1	0
5	3	3	3	0
6	3	3	3	0
7	9	11	7	2
8	14	18	10	4
9	38	55	21	17
10	77	122	32	45
11	203	345	61	142
12	481	862	100	381
13	1,299	2,412	186	1,113
14	3,385	6,459	311	3,074
15	9,347	18,127	567	8,780
16	25,691	50,412	970	24,721
17	72,505	143,255	1,755	70,750
18	205,326	407,623	3,029	202,297
19	589,612	1,173,770	5,454	584,158
20	1,702,022	3,394,549	9,495	1,692,527

[a]The numbers of unbalanced 3D-trees are obtained under several conditions, i.e., $U_k^{(AC)}$: achiral and chiral unbalanced 3D-trees, where a pair of enantiomers is counted just once, $U_k^{(AC^2)}$: achiral and chiral unbalanced 3D-trees, where two enantiomers of each pair are counted separately; $U_k^{(A)}$: achiral unbalanced 3D-trees, and $U_k^{(C)}$: chiral unbalanced 3D-trees, where each pair of enantiomers is counted just once.

separately. Then, a generating function for enumerating them can be written as follows:

$$\widehat{U}(x)^{(AC^2)} = \sum_{k=1}^{\infty} \widehat{U}_k^{(AC^2)} x^k. \tag{73}$$

The generating function is obtained by applying equation 5 to this case, i.e.,

$$\widehat{U}(x)^{(AC^2)} = G(x)^{(AC^2)} - \widehat{C}(x)^{(AC^2)}. \tag{74}$$

By introducing equations 28 and 60 into this equation, we obtain the following functional equation:

$$\widehat{U}(x)^{(AC^2)} = \frac{x}{12}\left\{b(x)^4 + 3b(x^2)^2 + 8b(x)b(x^3)\right\} - \frac{1}{2}\left\{(b(x)-1)^2 + (b(x^2)-1)\right\}. \tag{75}$$

After the ligand inventories shown in equations 12–14 are introduced into equation 75, the resulting equation is expanded to give a generating function:

$$\begin{aligned}\widehat{U}(x)^{(AC^2)} = {} & x + x^3 + x^4 + 3x^5 + 3x^6 + 11x^7 + 19x^8 + 55x^9 + 125x^{10} \\ & + 345x^{11} + 872x^{12} + 2412x^{13} + 6489x^{14} + 18127x^{15} + 50500x^{16} \\ & + 143255x^{17} + 407878x^{18} + 1173770x^{19} + 3395291x^{20} + \cdots . \end{aligned} \quad (76)$$

Let $U_k^{(AC^2)}$ be the (corrected) number of inequivalent achiral unbalanced promolecules (or 3D-trees) plus inequivalent chiral unbalanced promolecules (or 3D-trees) of carbon content k, where two enantiomers of each pair are counted separately. Then, a generating function for enumerating them can be written as follows:

$$U(x)^{(AC^2)} = \sum_{k=1}^{\infty} U_k^{(AC^2)} x^k. \quad (77)$$

The generating function is obtained by applying equation 5 to this case, i.e.,

$$U(x)^{(AC^2)} = G(x)^{(AC^2)} - C(x)^{(AC^2)} \quad (78)$$

into which equations 48 and 60 are introduced so as to give the following functional equation:

$$\begin{aligned} U(x)^{(AC^2)} = {} & \frac{x}{12}\left\{b(x)^4 + 3b(x^2)^2 + 8b(x)b(x^3)\right\} \\ & - \frac{1}{2}\left\{(b(x)-1)^2 + (b(x^2)-1)\right\} - \frac{1}{2}\left\{(c(x^2)-1) - (a(x^2)-1)\right\}. \end{aligned} \quad (79)$$

After the ligand inventories shown in equations 12–14 are introduced into equation 79, the resulting equation is expanded to give a generating function. The coefficient of the term x^k is the value of $U_k^{(AC)}$, which are shown up to carbon content 20 in the corresponding column of table 1.

Let $\widehat{U}_k^{(A)}$ be the uncorrected number of inequivalent achiral unbalanced promolecules of carbon content k, which appears as each coefficient of the following generating function:

$$\widehat{U}(x)^{(A)} = \sum_{k=0}^{\infty} \widehat{U}_k^{(A)} x^k. \quad (80)$$

The generating function is obtained by applying equation 5 to this case, i.e.,

$$\widehat{U}(x)^{(A)} = G(x)^{(A)} - \widehat{C}(x)^{(AC)}. \quad (81)$$

This equation is converted into the following functional equation by using equations 32 and 64, i.e.,

$$\widehat{U}(x)^{(A)} = \frac{x}{2}\left\{a(x)^2 c(x^2) + c(x^4)\right\} - \frac{1}{2}\left\{(a(x)-1)^2 + (c(x^2)-1)\right\}. \tag{82}$$

The ligand inventories shown in equations 12–14 are introduced into equation 82 and the resulting equation is expanded to give the following generating function:

$$\begin{aligned}\widehat{U}(x)^{(A)} = {} & x + x^3 + x^4 + 3x^5 + 3x^6 + 7x^7 + 9x^8 + 21x^9 + 29x^{10} \\ & + 61x^{11} + 90x^{12} + 186x^{13} + 281x^{14} + 567x^{15} + 882x^{16} \\ & + 1755x^{17} + 2774x^{18} + 5454x^{19} + 8753x^{20} + \cdots\end{aligned} \tag{83}$$

Let $U_k^{(A)}$ be the (corrected) number of inequivalent achiral unbalanced promolecules of carbon content k, which appears as each coefficient of the following generating function:

$$U(x)^{(A)} = \sum_{k=0}^{\infty} U_k^{(A)} x^k. \tag{84}$$

The generating function is obtained by applying equation 5 to this case, i.e.,

$$U(x)^{(A)} = G(x)^{(A)} - C(x)^{(A)}. \tag{85}$$

By considering equations 36 and 64, we obtain the following functional equation:

$$U(x)^{(A)} = \frac{x}{2}\left\{a(x)^2 c(x^2) + c(x^4)\right\} - \frac{1}{2}\left\{(a(x)-1)^2 + (a(x^2)-1)\right\}. \tag{86}$$

The ligand inventories shown in equations 12–14 are introduced into equation 86. After the expansion of the resulting equation, the coefficient $U_k^{(A)}$ of each term x^k is collected up to carbon content 20 in the corresponding column of table 1.

Let $\widehat{U}_k^{(C)}$ be the uncorrected number of inequivalent chiral unbalanced promolecules (or 3D-trees), where each pair of two enantiomers is counted just once. The corresponding generating function for enumerating them is represented as follows:

$$\widehat{U}(x)^{(C)} = \sum_{k=0}^{n} \widehat{U}_k^{(C)} x^k. \tag{87}$$

The generating function is obtained by applying equation 5 to this case, i.e.,

$$\widehat{U}(x)^{(C)} = G(x)^{(C)} - \widehat{C}(x)^{(C)}. \tag{88}$$

By starting from equations 40 and 68, we obtain the following functional equation:

$$\widehat{U}(x)^{(C)} = \frac{x}{24}\left\{b(x)^4 + 3b(x^2)^2 + 8b(x)b(x^3) - 6a(x)^2c(x^2) - 6c(x^4)\right\} - \frac{1}{4}\left\{(b(x)-1)^2 + (b(x^2)-1) - (a(x)-1)^2 - (c(x^2)-1)\right\}. \quad (89)$$

The ligand inventories shown in equations 12–14 are introduced into equation 89 and the resulting equation is expanded to give the following generating function:

$$\widehat{U}(x)^{(C)} = 2x^7 + 5x^8 + 17x^9 + 48x^{10} + 142x^{11} + 391x^{12} + 1113x^{13} + 3104x^{14} + 8780x^{15} + 24809x^{16} + 70750x^{17} + 202552x^{18} + 584158x^{19} + 1693269x^{20} + \cdots \quad (90)$$

Let $U_k^{(C)}$ be the (corrected) number of chiral unbalanced promolecules (or 3D-trees), where each pair of two enantiomers is counted just once. The corresponding generating function for enumerating them is represented as follows:

$$U(x)^{(C)} = \sum_{k=0}^{\infty} U_k^{(C)} x^k. \quad (91)$$

The generating function is obtained by applying equation 5 to this case, i.e.,

$$U(x)^{(C)} = G(x)^{(C)} - C(x)^{(C)} \quad (92)$$

into which equations 44 and 68 are introduced so as to give the following functional equation:

$$U(x)^{(C)} = \frac{x}{24}\left\{b(x)^4 + 3b(x^2)^2 + 8b(x)b(x^3) - 6a(x)^2c(x^2) - 6c(x^4)\right\} - \frac{1}{4}\left\{(b(x)-1)^2 + (b(x^2)-1) - (a(x)-1)^2 + (c(x^2)-1) - 2(a(x^2)-1)\right\}. \quad (93)$$

The ligand inventories shown in equations 12–14 are introduced into equation 93. After the expansion of the resulting equation, the coefficient $U_k^{(C)}$ of each term x^k is collected up to carbon content 20 in the corresponding column of table 1.

3.3. Enumeration of balanced 3D-trees

Balanced 3D-trees are represented by X–X, p–p ($\overline{p}$–$\overline{p}$), or p–$\overline{p}$, as shown in figure 5. Among the terms appearing in equation 22, the terms for 2-cycles (i.e., b_2 and c_2) are selected to characterize these three types:

$$\frac{1}{2}\left(b_2 + c_2\right), \tag{94}$$

where the top fraction (1/2) represents the average of the results due to the two terms at issue.

Let $B_k^{(AC)}$ be the number of inequivalent balanced 3D-trees of carbon content k, which are achiral ones plus enantiomeric pairs of chiral ones. Each $B_k^{(AC)}$ appears in the following generating function:

$$B(x)^{(AC)} = \sum_{k=1}^{\infty} B_k^{(AC)} x^k. \tag{95}$$

By replacing a_d, c_d, and b_d by $a(x^d) - 1$, $c(x^d) - 1$, and $b(x^d) - 1$, respectively, equation 94 is converted into the corresponding functional equation as follows:

$$B(x)^{(AC)} = \frac{1}{2}\left\{\left(b(x^2) - 1\right) + \left(c(x^2) - 1\right)\right\}. \tag{96}$$

The ligand inventories shown in equations 13 and 14 are introduced into equation 96. After the expansion of the resulting equation, the coefficient $B_k^{(AC)}$ of each term x^k is collected up to carbon content 20 in the corresponding column of table 2.

Let $\widehat{B}_k^{(AC^2)}$ be the uncorrected number of inequivalent balanced 3D-trees of carbon content k, which are achiral and chiral.

$$\widehat{B}(x)^{(AC^2)} = \sum_{k=1}^{\infty} \widehat{B}_k^{(AC^2)} x^k. \tag{97}$$

Because the term for a 2-cycle appearing in equation 26 is b_2, it is replaced by $b(x^2) - 1$. Thereby, the corresponding functional equation is obtained as follows:

$$\widehat{B}(x)^{(AC^2)} = b(x^2) - 1. \tag{98}$$

The ligand inventory shown in equation 14 is introduced into equation 98.

$$\begin{aligned}\widehat{B}(x)^{(AC^2)} = {} & x^2 + x^4 + 2x^6 + 5x^8 + 11x^{10} + 28x^{12} + 74x^{14} \\ & + 199x^{16} + 551x^{18} + 1553x^{20} + \cdots .\end{aligned} \tag{99}$$

Table 2
The numbers of balanced 3D-trees or alkanes[a].

k	$B_k^{(AC)}$	$B_k^{(AC^2)}$	$B_k^{(A)}$	$B_k^{(C)}$
2	1	1	1	0
4	1	1	1	0
6	2	2	2	0
8	5	6	4	1
10	11	14	8	3
12	28	38	18	10
14	74	104	44	30
16	199	287	111	88
18	551	806	296	255
20	1,553	2,295	811	742

[a]The numbers of balanced 3D-trees are obtained under several conditions, i.e., $B_k^{(AC)}$: achiral and chiral balanced 3D-trees, where a pair of enantiomers is counted just once, $B_k^{(AC^2)}$: achiral and chiral balanced 3D-trees, where two enantiomers of each pair are counted separately, $B_k^{(A)}$: achiral balanced 3D-trees, and $B_k^{(C)}$: chiral balanced 3D-trees, where each pair of enantiomers is counted just once.

Let $\widehat{B}_k^{(A)}$ be the uncorrected number of inequivalent balanced 3D-trees of carbon content k, which are achiral.

$$\widehat{B}(x)^{(A)} = \sum_{k=1}^{\infty} \widehat{B}_k^{(A)} x^k. \tag{100}$$

Because the terms for 2-cycles appearing in equation 30 is c_2, it is replaced by $c(x^2) - 1$. Thereby, the corresponding functional equation is obtained as follows:

$$\widehat{B}(x)^{(A)} = c(x^2) - 1. \tag{101}$$

The ligand inventory shown in equation 13 is introduced into equation 98 to give the following generating function:

$$\begin{aligned}\widehat{B}(x)^{(A)} = {} & x^2 + x^4 + 2x^6 + 5x^8 + 11x^{10} + 28x^{12} + 74x^{14} \\ & + 199x^{16} + 551x^{18} + 1553x^{20} + \cdots .\end{aligned} \tag{102}$$

Alternatively, achiral balanced 3D-trees are represented by X–X or p–$\overline{\text{p}}$, as exemplified in figure 5. They are in agreement with the terms for 2-cycles (i.e., a_2 and c_2). On the analogy of the derivation of equation 94, we obtain the following CI-CF:

$$\frac{1}{2}\left(a_2 + c_2\right), \tag{103}$$

where the top fraction (1/2) represents the average of the results due to the two terms at issue.

Let $B_k^{(A)}$ be the (corrected) number of inequivalent balanced 3D-trees of carbon content k, which are achiral. Each $B_k^{(A)}$ appears in the following generating function:

$$B(x)^{(A)} = \sum_{k=1}^{\infty} B_k^{(A)} x^k. \tag{104}$$

By replacing a_d and c_d by $a(x^d) - 1$ and $c(x^d) - 1$, equation 103 is converted into the corresponding functional equation as follows:

$$B(x)^{(A)} = \frac{1}{2}\left\{(a(x^2) - 1) + (c(x^2) - 1)\right\}. \tag{105}$$

The ligand inventories shown in equations 12 and 13 are introduced into equation 105. After the expansion of the resulting equation, the coefficient $B_k^{(A)}$ of each term x^k is collected up to carbon content 20 in the corresponding column of table 2.

The subtraction of c_2 from equation 94 gives the following CI-CF:

$$\frac{1}{2}(b_2 - c_2). \tag{106}$$

Let $\widehat{B}_k^{(C)}$ be the (uncorrected) number of inequivalent balanced 3D-trees of carbon content k, which are chiral. Each $\widehat{B}_k^{(C)}$ appears in the following generating function:

$$\widehat{B}(x)^{(C)} = \sum_{k=1}^{\infty} \widehat{B}_k^{(C)} x^k. \tag{107}$$

By replacing b_d and c_d by $b(x^d) - 1$ and $c(x^d) - 1$, equation 106 is converted into the corresponding functional as follows:

$$\widehat{B}(x)^{(C)} = \frac{1}{2}\left\{(b(x^2) - 1) - (c(x^2) - 1)\right\}, \tag{108}$$

which is also obtained by the subtraction $\widehat{B}(x)^{(C)} = B(x)^{(AC)} - \widehat{B}(x)^{(A)}$ (cf. equations 96 and 98). Because the present enumeration is concerned with carbon contents, the value $\widehat{B}(x)^{(C)}$ usually vanishes, i.e.,

$$\widehat{B}(x)^{(C)} = 0. \tag{109}$$

The subtraction of equation 103 from 94 gives the following CI-CF:

$$\frac{1}{2}(b_2 - a_2). \tag{110}$$

Let $B_k^{(C)}$ be the corrected number of inequivalent balanced 3D-trees of carbon content k, which are chiral. Each $B_k^{(C)}$ appears in the following generating function:

$$B(x)^{(C)} = \sum_{k=1}^{\infty} B_k^{(C)} x^k. \tag{111}$$

By replacing a_d and b_d by $a(x^d) - 1$ and $b(x^d) - 1$, equation 110 is converted into the corresponding counting series as follows:

$$B(x)^{(C)} = \frac{1}{2}\left\{(b(x^2) - 1) - (a(x^2) - 1)\right\}. \tag{112}$$

The ligand inventories shown in equations 12 and 14 are introduced into equation 112. After the expansion of the resulting equation, the coefficient $B_k^{(C)}$ of each term x^k is collected up to carbon content 20 in the corresponding column of table 2.

Let $B_k^{(AC^2)}$ be the (corrected) number of inequivalent balanced 3D-trees of carbon content k, which are achiral and chiral.

$$B(x)^{(AC^2)} = \sum_{k=1}^{\infty} B_k^{(AC^2)} x^k. \tag{113}$$

To evaluate $B(x)^{(AC^2)}$, we sum up equations 94 and 110 to give:

$$\frac{1}{2}(b_2 + c_2) + \frac{1}{2}(b_2 - a_2) = b_2 + \frac{1}{2}(c_2 - a_2). \tag{114}$$

By replacing a_d, c_d, and b_d by $a(x^d) - 1$, $c(x^d) - 1$, and $b(x^d) - 1$, respectively, equation 94 is converted into the corresponding functional equation as follows:

$$B(x)^{(AC^2)} = (b(x^2) - 1) + \frac{1}{2}\left\{(c(x^2) - 1) - (a(x^2) - 1)\right\}. \tag{115}$$

The ligand inventories shown in equations 12–14 are introduced into equation 115. The resulting coefficient $B_k^{(AC^2)}$ are collected up to carbon content 20 in the corresponding column of table 2.

The corrected and uncorrected functional equations for evaluating balanced 3D-trees satisfy the following relationships:

$$B(x)^{(AC)} = B(x)^{(A)} + B(x)^{(C)}, \tag{116}$$
$$B(x)^{(AC)} = \widehat{B}(x)^{(A)} + \widehat{B}(x)^{(C)}, \tag{117}$$

$$B(x)^{(AC^2)} = B(x)^{(AC)} + B(x)^{(C)}, \tag{118}$$
$$\widehat{B}(x)^{(AC^2)} = B(x)^{(AC)} + \widehat{B}(x)^{(C)}. \tag{119}$$

Thus, equation 116 is derived from equations 96, 105, and 112 (cf. table 2); and equation 117 is derived from equations 96, 101, and 108 or alternatively from the data of table 2, 102, and 109. On the other hand, equation 118 is derived from equations 115, 96, and 112 (cf., table 2); and equation 119 is derived from equation 98, 96, and 108 or alternatively from equation 99, the data of table 2, and equation 109.

3.4. Enumeration of 3D-trees

3.4.1. Adjusted contaminants

Because the number of unbalanced 3D-trees and the number of balanced 3D-trees have been obtained under the four conditions, the addition of them gives the net number of 3D-trees, i.e.,

$$N(x) = U(x) + B(x) = G(x) - C(x) + B(x), \tag{120}$$

where the superscripts showing the conditions are omitted. In order to obtain the $N(x)$, we define $A(x)$ for evaluating adjusted contaminants as follows:

$$A(x) = C(x) - B(x). \tag{121}$$

Thereby, we can place

$$N(x) = G(x) - A(x). \tag{122}$$

According to the four conditions, we obtain the following functional equations for evaluating adjusted contaminants:

$$\begin{aligned} A(x)^{(AC)} &= C(x)^{(AC)} - B(x)^{(AC)} \\ &= \frac{1}{4}\left\{(b(x)-1)^2 - (b(x^2)-1) + (a(x)-1)^2 - (c(x^2)-1)\right\}, \end{aligned} \tag{123}$$

$$\begin{aligned} A(x)^{(AC^2)} &= \widehat{C}(x)^{(AC^2)} - \widehat{B}(x)^{(AC^2)} \\ &= C(x)^{(AC^2)} - B(x)^{(AC^2)} \\ &= \frac{1}{2}\left\{(b(x)-1)^2 - (b(x^2)-1)\right\}, \end{aligned} \tag{124}$$

$$\begin{aligned} A(x)^{(A)} &= \widehat{C}(x)^{(A)} - \widehat{B}(x)^{(A)} \\ &= C(x)^{(A)} - B(x)^{(A)} \\ &= \frac{1}{2}\left\{(a(x)-1)^2 - (c(x^2)-1)\right\}, \end{aligned} \tag{125}$$

$$\begin{aligned} A(x)^{(C)} &= \widehat{C}(x)^{(C)} - \widehat{B}(x)^{(C)} \\ &= C(x)^{(C)} - B(x)^{(C)} \\ &= \frac{1}{4}\left\{(b(x)-1)^2 - (b(x^2)-1) - (a(x)-1)^2 + (c(x^2)-1)\right\}. \end{aligned} \tag{126}$$

Thus, equation 123 is obtained by using equations 24 and 96; equation 124 is obtained by using equations 28 and 98 or by using equations 48 and 115; equation 125 is obtained by using equations 32 and 101 or by using equations 36 and 105; and 126 is obtained by using equations 40 and 108 or by using equations 44 and 112.

3.4.2. 3D-trees

Because $G(x)$ and $A(x)$ have been evaluated under the four conditions in the preceding discussions, we are able to obtain $N(x)$ according to equation 122:

Theorem 7. Let $G(x)$ (equation 2) be a generating function for counting inequivalent uninuclear promolecules. Let $A(x)$ (equation 121) be a generating function for counting inequivalent adjusted contaminants. Then, the subtraction $N(x) = G(x) - A(x)$ (equation 122) gives the numbers of inequivalent 3D-trees as its coefficients. Thus, the coefficients satisfy the relationship $N_k = G_k - A_k$ (k: nonnegative integers).

Let $N_k^{(AC)}$ be the number of inequivalent achiral promolecules (or 3D-trees) plus inequivalent enantiomeric pairs of chiral promolecules (or 3D-trees) of carbon content k. Then, a generating function for enumerating them can be written as follows:

$$N(x)^{(AC)} = \sum_{k=1}^{\infty} N_k^{(AC)} x^k. \tag{127}$$

The generating function is obtained by applying equation 122 to this case, i.e.,

$$N(x)^{(AC)} = G(x)^{(AC)} - A(x)^{(AC)}. \tag{128}$$

Hence, we obtain the following functional equation from equations 24 and 123, i.e,

$$\begin{aligned} N(x)^{(AC)} = {} & \frac{x}{24}\left\{b(x)^4 + 3b(x^2)^2 + 8b(x)b(x^3) + 6a(x)^2c(x^2) + 6c(x^4)\right\} \\ & -\frac{1}{4}\left\{(b(x)-1)^2 - (b(x^2)-1) + (a(x)-1)^2 - (c(x^2)-1)\right\}. \end{aligned} \tag{129}$$

Let $N_k^{(AC^2)}$ be the number of inequivalent achiral promolecules (or 3D-trees) plus inequivalent chiral promolecules (or 3D-trees) of carbon content k, where two enantiomers of each pair are counted separately. Then, a generating function for enumerating them can be written as follows:

$$N(x)^{(AC^2)} = \sum_{k=1}^{\infty} N_k^{(AC^2)} x^k. \tag{130}$$

The generating function is obtained by applying equation 122 to this case, i.e.,

$$N(x)^{(AC^2)} = G(x)^{(AC^2)} - A(x)^{(AC^2)}. \tag{131}$$

By considering equations 28 and 124, we obtain the following functional equation:

$$N(x)^{(AC^2)} = \frac{x}{12}\left\{b(x)^4 + 3b(x^2)^2 + 8b(x)b(x^3)\right\} - \frac{1}{2}\left\{(b(x)-1)^2 - (b(x^2)-1)\right\}. \tag{132}$$

Let $N_k^{(A)}$ be the number of inequivalent achiral promolecules of carbon content k, which appears as each coefficient of the following generating function:

$$N(x)^{(A)} = \sum_{k=0}^{\infty} N_k^{(A)} x^k. \tag{133}$$

The generating function is obtained by applying equation 122 to this case, i.e.,

$$N(x)^{(A)} = G(x)^{(A)} - A(x)^{(A)}. \tag{134}$$

This equation is combined with equations 36 and 125 to give the following functional equation:

$$N(x)^{(A)} = \frac{x}{2}\left\{a(x)^2 c(x^2) + c(x^4)\right\} - \frac{1}{2}\left\{(a(x)-1)^2 - (c(x^2)-1)\right\}. \tag{135}$$

This equation is further transformed into a simpler one by using equation 9.

$$N(x)^{(A)} = \frac{1}{2}\left\{a(x) + xc(x^4) + c(x^2)\right\} - 1. \tag{136}$$

Let $N_k^{(C)}$ be the number of inequivalent chiral promolecules (or 3D-trees), where each pair of two enantiomers is counted just once. The corresponding generating function for enumerating them is represented as follows:

$$N(x)^{(C)} = \sum_{k=0}^{\infty} N_k^{(C)} x^k. \tag{137}$$

The generating function is obtained by applying equation 122 to this case, i.e.,

$$N(x)^{(C)} = G(x)^{(C)} - A(x)^{(C)}. \tag{138}$$

This equation is modified by equations 44 and 126 to give the following functional equation:

$$N(x)^{(C)} = \frac{x}{24}\{b(x)^4 + 3b(x^2)^2 + 8b(x)b(x^3) - 6a(x)^2c(x^2) - 6c(x^4)\} - \frac{1}{4}\left\{(b(x)-1)^2 - (b(x^2)-1) - (a(x)-1)^2 + (c(x^2)-1)\right\}. \quad (139)$$

The ligand inventories shown in equations 12–14 are introduced into equations 129, 132, 135, 136, and 139. After the expansion of the resulting equations, the coefficients of the terms x^k under the respective conditions are collected up to carbon content 20 in the corresponding columns of table 3. As found by the derivation procedure, the values collected in table 3 are alternatively obtained by summing up the corresponding values collected in tables 1 and 2. In addition, they satisfy the following equations:

$$N(x)^{(AC)} = N(x)^{(A)} + N(x)^{(C)}, \quad (140)$$

$$N(x)^{(AC^2)} = N(x)^{(AC)} + N(x)^{(C)}, \quad (141)$$

as found in table 3.

4. Discussions

4.1. Comments on contaminants and balanced 3D-trees

4.1.1. Uninuclear and binuclear 3D-trees for characterizing a 3D-tree of meso-type

The comparison between equations 33 ($\widehat{C}(x)^{(A)}$) and 37 ($C(x)^{(A)}$) provides us with a deeper insight to how 3D-trees of *meso*-type participate in enumeration as contaminants. For example, the coefficient of the term x^8 of equation 33 ($\widehat{C}(x)^{(A)}$) is equal to 39, while the corresponding coefficient in equation 37 is equal to 38. The difference 1 (=39 − 38) comes from whether the *meso*-3D-tree (**36**) is counted as an achiral 3D-tree or not. This point shall be discussed in detail, where the relationship between uninuclear promolecules and binuclear promolecules for the *meso*-3D-tree (**36**) shall be clarified especially with respect to their chiralities or achiralities. For this purpose, figure 7 is redrawn into figure 11.

Let us first examine the enumeration result based on equation 64 for $G(x)^{(A)}$. The enumeration result involves an irregular specification with respect to the achirality of the *meso*-3D-tree (**36**), because it is concerned only with carbon contents. This irregularity can be clarified by the following treatment.

The uninuclear promolecules (**49**–**52** shown in figure 11) for the *meso*-3D-tree (**36**) are generated from the tetrahedral uninuclear skeleton (**30**) by placing four proligands selected from a set of proligands:

$$\mathbf{X} = \{\mathrm{H}, \mathrm{X}_1, \mathrm{X}_2; \mathrm{p}_1, \mathrm{p}_2, \mathrm{p}_3, \mathrm{p}_4; \overline{\mathrm{p}}_1, \overline{\mathrm{p}}_2, \overline{\mathrm{p}}_3, \overline{\mathrm{p}}_4\}, \quad (142)$$

Table 3
The numbers of 3D-trees or alkanes[a].

k	$N_k^{(AC)}$	$N_k^{(AC^2)}$	$N_k^{(A)}$	$N_k^{(C)}$
1	1	1	1	0
2	1	1	1	0
3	1	1	1	0
4	2	2	2	0
5	3	3	3	0
6	5	5	5	0
7	9	11	7	2
8	19	24	14	5
9	38	55	21	17
10	88	136	40	48
11	203	345	61	142
12	509	900	118	391
13	1,299	2,412	186	1,113
14	3,459	6,563	355	3,104
15	9,347	18,127	567	8,780
16	25,890	50,699	1,081	24,809
17	72,505	143,255	1,755	70,750
18	205,877	408,429	3,325	202,552
19	589,612	1,173,770	5,454	584,158
20	1,703,575	3,396,844	10,306	1,693,269

[a]The numbers of 3D-trees are obtained under several conditions, i.e., $N_k^{(AC)}$: achiral and chiral 3D-trees, where a pair of enantiomers is counted just once, $N_k^{(AC^2)}$: achiral and chiral 3D-trees, where two enantiomers of each pair are counted separately, $N_k^{(A)}$: achiral 3D-trees, and $N_k^{(C)}$: chiral 3D-trees, where each pair of enantiomers is counted just once.

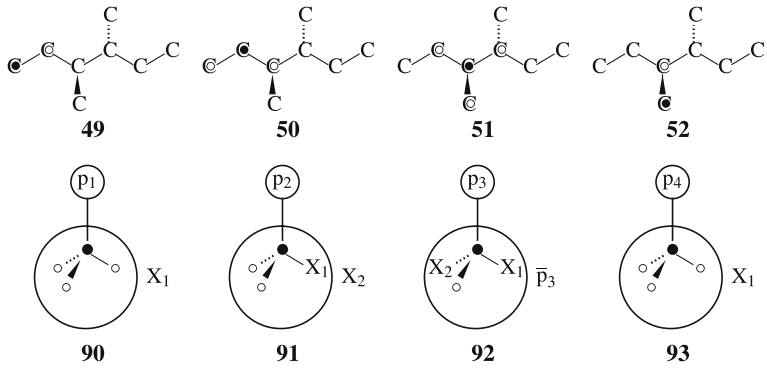

Figure 11. Uninuclear and binuclear 3D-trees for characterizing a 3D-tree of *meso*-type.

where the symbols are used to represent as follows:

$$\begin{aligned}
\mathrm{H} &= \mathrm{H}\ \text{(hydrogen)} && x^0,\\
\mathrm{X}_1 &= \mathrm{CH_3} && x,\\
\mathrm{X}_2 &= \mathrm{CH_2CH_3} && x^2,\\
\mathrm{p}_1, \overline{\mathrm{p}}_1 &= \textit{RS}\text{- or } \textit{SR}\text{-}\mathrm{CH_2CH(CH_3)CH(CH_3)CH_2CH3} && x^7,\\
\mathrm{p}_2, \overline{\mathrm{p}}_2 &= \textit{RS}\text{- or } \textit{SR}\text{-}\mathrm{CH(CH_3)CH(CH_3)CH_2CH3} && x^6,\\
\mathrm{p}_3, \overline{\mathrm{p}}_3 &= \textit{S}\text{- or } \textit{R}\text{-}\mathrm{CH(CH_3)CH_2CH3} && x^4,\\
\mathrm{p}_4, \overline{\mathrm{p}}_4 &= \textit{RS}\text{- or } \textit{SR}\text{-}\mathrm{CH(CH_2CH_3)CH(CH_3)CH_2CH3} && x^7.
\end{aligned} \tag{143}$$

According to these expressions, the uninuclear 3D-tree (**49**) is expressed as $\mathrm{H^3p_1}$, which corresponds to the term $x \times (x^0)^3 \cdot x^7 = x^8$. Similarly, the uninuclear 3D-tree (**50**) is expressed as $\mathrm{H^2X_1p_2}$ ($x \times (x^0)^2 \cdot x \cdot x^6 = x^8$), **51** as $\mathrm{HX_1X_2p_3}$ ($x \times x^0 \cdot x \cdot x^2 \cdot x^4 = x^8$), as **52** as $\mathrm{H^3p_4}$ ($x \times (x^0)^3 \cdot x^7 = x^8$). It should be noted that these expressions indicate that the uninuclear 3D-trees are regarded as being chiral, whereas the corresponding *meso*-3D-tree (**36**) is achiral.

This irregular assignment is only apparent so as to be ascribed to the fact the enumeration based on the tetrahedral uninuclear skeleton (**30**) fixes the central vertex (•) as a core. The core is implicitly (or conceptually) differentiated from other non-terminal vertices during the enumeration. Chemically speaking, suppose that the nucleus is an isotopical carbon (^{13}C) and other non-terminal vertices are all ^{12}C, although the isotopes ^{12}C and ^{13}C are regarded as the same carbon atoms under several conditions.

The irregular assignment described in the preceding paragraphs can be more quantitatively explained by using Fujita's proligand method [16–18]. The ligand inventories for the set **X** (equation 142) are obtained as follows:

$$a_d = \mathrm{H}^d + \mathrm{X}_1^d + \mathrm{X}_2^2, \tag{144}$$

$$c_d = \mathrm{H}^d + \mathrm{X}_1^d + \mathrm{X}_2^2 + 2\mathrm{p}_1^{d/2}\overline{\mathrm{p}}_1^{d/2} + 2\mathrm{p}_2^{d/2}\overline{\mathrm{p}}_2^{d/2} + 2\mathrm{p}_3^{d/2}\overline{\mathrm{p}}_3^{d/2} + 2\mathrm{p}_4^{d/2}\overline{\mathrm{p}}_4^{d/2}, \tag{145}$$

$$b_d = \mathrm{H}^d + \mathrm{X}_1^d + \mathrm{X}_2^2 + \mathrm{p}_1^d + \overline{\mathrm{p}}_1^d + \mathrm{p}_2^d + \overline{\mathrm{p}}_2^d + \mathrm{p}_3^d + \overline{\mathrm{p}}_3^d + \mathrm{p}_4^d + \overline{\mathrm{p}}_4^d. \tag{146}$$

The number of achiral 3D-trees enumerate by equation 62 (corresponding to equation 64 for $G(x)^{(A)}$) is evaluated as follows:

$$\begin{aligned}
G_A = {} & [\mathrm{H}^4 + \mathrm{X}_1^4 + \mathrm{X}_2^4] + [\mathrm{H}^3X_1 + \mathrm{H}^3X_2 + \cdots]\\
& + [\mathrm{H}^2X_1^2 + \mathrm{H}^2X_2^2 + \cdots] + [\mathrm{H}^2X_1X_2 + \mathrm{H}X_1^2\mathrm{X}_2 + \cdots]\\
& + [\mathrm{H}^2\mathrm{p}_1\overline{\mathrm{p}}_1 + \mathrm{H}^2\mathrm{p}_2\overline{\mathrm{p}}_2 + \cdots] + [\mathrm{HX}_1\mathrm{p}_1\overline{\mathrm{p}}_1 + \mathrm{HX}_2\mathrm{p}_2\overline{\mathrm{p}}_2 + \cdots]\\
& + [\mathrm{p}_1^2\overline{\mathrm{p}}_1^2 + \mathrm{p}_2^2\overline{\mathrm{p}}_2^2 + \cdots],
\end{aligned} \tag{147}$$

which is obtained by introducing the ligand inventories (equations 144–146) into equation 62. The resulting generating function (equation 147) does not contain $\mathrm{H^3p_1}$ for **49**, $\mathrm{H^2X_1p_2}$ for **50**, $\mathrm{HX_1X_2p_3}$ for **51**, nor $\mathrm{H^3p_4}$ for **52**. Because

$HX_1X_2p_3$ corresponds to the achiral **51**, the evaluation by equation 147 results in the underestimation concerned with **51**.

On the other hand, the number of chiral 3D-trees enumerate by equation 66 (corresponding to equation 68 for $G(x)^{(C)}$) is evaluated by introducing the ligand inventories (equations 144–146) into equation 66. The resulting equation is expanded to give the following generating function:

$$G_C = \cdots + \frac{1}{2}\left(H^3p_1 + H^3\overline{p}_1\right)\cdots + \frac{1}{2}\left(H^2X_1p_2 + H^2X_1\overline{p}_2\right)\cdots + \left(HX_1X_2p_3 + HX_1X_2\overline{p}_3\right)\cdots + \frac{1}{2}\left(H^3p_4 + H^3\overline{p}_4\right)\cdots, \quad (148)$$

where other terms are omitted so as to leave only necessary terms. Thus, the resulting generating function (equation 148) contains H^3p_1 ($H^3\overline{p}_1$) for **49**, $H^2X_1p_2$ ($H^2X_1\overline{p}_2$) for **50**, and H^3p_4 ($H^3\overline{p}_4$) for **52**. The term ($HX_1X_2p_3$ + $HX_1X_2\overline{p}_3$) should be divided into two parts, i.e., the term corresponding to $p_3\overline{p}_3$ for the *meso*-3D-tree (**51**) and the term $\frac{1}{2}\left(p_3^2 + \overline{p}_3^2\right)$ for the enantiomeric pair (**50/$\overline{\mathbf{50}}$**). Note that the term $p_3\overline{p}_3$ should be regarded as $\frac{1}{2}\left(p_3\overline{p}_3 + \overline{p}_3p_3\right)$, because $p_3\overline{p}_3$ and $\overline{p}_3p_3$ are regarded irregularly as enantiomers and counted as a pair of enantiomers in the enumeration as uninuclear promolecules. Because $HX_1X_2p_3$ corresponds to the achiral **51**, the evaluation by equation 148 results in the overestimation concerned with **51**.

Let us consider that the binuclear promolecules (**90**–**93** shown in figure 11) for the *meso*-3D-tree (**36**) are generated from the binuclear skeleton (**31**) by placing two proligands selected from the set (**X**) shown in equation 142. The number of achiral 3D-trees enumerated by equation 30 (corresponding to equation 32 for $\widehat{C}(x)^{(A)}$) is evaluated by introducing the ligand inventories (equations 144–146) into equation 30. The resulting equation is expanded to give the following generating function:

$$\widehat{C}_A = \left[H^2 + X_1^2 + X_2^2\right] + [HX_1 + HX_2 + X_1X_2] + [p_1\overline{p}_1 + p_2\overline{p}_2 + p_3\overline{p}_3 + p_4\overline{p}_4], \quad (149)$$

which contains the term $p_3\overline{p}_3$ for **92** (corresponding to **51**). Because the presence of the term $p_3\overline{p}_3$ in equation 149 correctly specifies the achirality of **92**, the underestimation due to the absence of the term $p_3\overline{p}_3$ in G_A (equation 147) cannot be corrected by equation 149.

The corrected functional equation corresponding to equation 149 is calculated by introducing the ligand inventories (equations 144–146) into equation 34 as follows:

$$C_A = [H^2 + X_1^2 + X_2^2] + [HX_1 + HX_2 + X_1X_2], \quad (150)$$

which does not contain the term $p_3\overline{p}_3$ for **92** (corresponding to **51**). Although equation 150 gives a rather erroneous specification of the achirality of **92**, it can correct the underestimation of G_A (equation 147).

The number of chiral 3D-trees enumerated by equation 38 (corresponding to equation 40 for $\widehat{C}(x)^{(C)}$) is evaluated by introducing the ligand inventories (equations 144–146) into equation 38. The resulting equation is expanded to give the following generating function:

$$\widehat{C}_C = \frac{1}{2}\left(X_1p_1 + X_1\overline{p}_1\right)\cdots + \frac{1}{2}\left(X_3p_2 + X_3\overline{p}_2\right)\cdots + \frac{1}{2}\left(X_1p_4 + X_1\overline{p}_4\right)\cdots + \frac{1}{2}\left(p_3^2 + \overline{p}_3^2\right)\cdots, \tag{151}$$

where other terms are omitted so as to leave only necessary terms. Thus, the resulting generating function (equation 151) contains the term X_1p_1 ($X_1\overline{p}_1$) for **90** (cf. **49**), the term X_3p_2 ($X_3\overline{p}_2$) for **91** (cf. **50**), and the term X_1p_4 ($X_1\overline{p}_4$) for **93** (cf. **52**); and it does not contain the term $p_3\overline{p}_3$ for **92** (cf. **51**) but contains the term $\frac{1}{2}\left(p_3^2 + \overline{p}_3^2\right)$ for the enantiomeric pair (**50**/$\overline{\mathbf{50}}$). Because equation 151 correctly specifies the achirality of **92** by the absence of the term $p_3\overline{p}_3$, it cannot correct the overestimation of G_C (equation 148).

The corrected functional equation corresponding to equation 151 is calculated by introducing the ligand inventories (equations 144–146) into equation 42 as follows:

$$C_C = \frac{1}{2}\left(X_1p_1 + X_1\overline{p}_1\right)\cdots + \frac{1}{2}\left(X_3p_2 + X_3\overline{p}_2\right)\cdots + \frac{1}{2}\left(X_1p_4 + X_1\overline{p}_4\right)\cdots + \frac{1}{2}\left(p_3^2 + \overline{p}_3^2\right)\cdots + p_3\overline{p}_3\cdots, \tag{152}$$

which contains the term $p_3\overline{p}_3$ for the achiral promolecule **92** (cf. **51**) as well as the term $\frac{1}{2}\left(p_3^2 + \overline{p}_3^2\right)$ for the enantiomeric pair (**50**/$\overline{\mathbf{50}}$). Although equation 152 erroneously specifies the achirality of **92**, it can correct the overestimation of G_C (equation 148).

The evaluation of the 3D-Tree of *meso*-type ($p_3\overline{p}_3$) and the related enantiomeric pair ($\frac{1}{2}(p_3^2 + \overline{p}_3^2)$) is summarized in table 4. The combination of equations 149 and 151 and that of equations 150 and 152 give the following equations:

$$C_{AC} = \widehat{C}_A + \widehat{C}_C, \tag{153}$$

$$C_{AC} = C_A + C_C, \tag{154}$$

which correspond to equations 50 and 51. Note that the C_{AC} is obtained by introducing the ligand inventories (equations 144–146) into equation 22 corresponding to equation 24.

The results described above are restated by referring to carbon contents. The evaluation of the number of achiral unbalanced 3D-trees in terms of G_A

Table 4
Evaluation of a 3D-tree of *meso*-type and the related enantiomeric pair.

	Uninuclear			Binuclear				
	$G(x)^{(AC)}$	$G(x)^{(A)}$	$G(x)^{(C)}$	$C(x)^{(AC)}$	$\widehat{C}(x)^{(A)}$	$\widehat{C}(x)^{(C)}$	$C(x)^{(A)}$	$C(x)^{(C)}$
	G_{AC}	G_A	G_C	C_{AC}	$\widehat{C}_A$	$\widehat{C}_C$	C_A	C_C
$p_3\overline{p}_3$	1	0	1	1	1	0	0	1
$\frac{1}{2}(p_3^2+\overline{p}_3^2)$	1	0	1	1	0	1	0	1
Contribution to x^8	2	0	2	2	1	1	0	2

(equation 147) $-\widehat{C}_A$ (equation 149) results in an overdrawn account by the term $p_3\overline{p}_3$. Hence the value $48x^8-39x^8=9x^8$ (equation 33 minus equation 41) fails in counting $p_3\overline{p}_3$ for **92** (cf. **51**). On the other hand, the evaluation of the number of chiral unbalanced 3D-trees in terms of G_C (equation 148) $-\widehat{C}_C$ (equation 151) results in overestimation by the term $p_3\overline{p}_3$. Hence, the value $55x^8-50x^8=5x^8$ (equation 69 − equation 41) counts unnecessary $p_3\overline{p}_3$ for **92** (cf. **51**).

It follows that the evaluation of the number of achiral and chiral unbalanced 3D-trees in terms of $G_{AC}-C_{AC}=(G_A+G_C)-(\widehat{C}_A+\widehat{C}_C)=(G_A-\widehat{C}_A)+(G_C-\widehat{C}_C)$ results in cancellation of the underestimation due to $(G_A-\widehat{C}_A)$ and the overestimation due to $(G_C-\widehat{C}_C)$. Hence, $U(x)^{(AC)}$ (equation 72) does not suffer from such under- nor overestimation, i.e., $(48-39)+(55-50)=14$, as collected in table 1.

4.1.2. Comments on balanced 3D-trees

The enumeration result based on equation 101 for $\widehat{B}(x)^{(A)}$ involves another type of irregular specification with respect to the *meso*-3D-tree (**36**), because it is concerned only with carbon contents. Thus, although the coefficient of the term x^8 in equation 102 is equal to 5, there are four achiral balanced 3D-trees, i.e., **32**–**36**, as shown in figure 5. This irregularity should be discussed in detail.

The ligand inventories (equations 144–146) are introduced into the cycle index c_2 corresponding to equation 101. Thereby, we obtain the following generating function:

$$\widehat{B}_A=H^2+X_1^2+X_2^2+2p_1\overline{p}_1+2p_2\overline{p}_2+2p_3\overline{p}_3+2p_4\overline{p}_4. \tag{155}$$

Among the terms appearing in the right-hand side of equation 155, the coefficient 2 of the term $p_3\overline{p}_3$ indicates that the term $p_3\overline{p}_3$ (corresponding to x^8) is regarded as an ordered pair and differentiated from the inverse pair $\overline{p}_3p_3$. Thus, the contribution of **36** to the term x^8 (via the term $p_3\overline{p}_3$) is doubly evaluated. Hence, the contribution of each balanced 3D-tree is found to be **32** (1), **33** (1), **34** (1), and **36** (2) so as to give $5x^8$ in equation 102.

To correct the irregularity of $\widehat{B}(x)^{(A)}$ (equation 101), we use equation 105 for $B(x)^{(A)}$. The ligand inventories (equations 144–146) are introduced into equation 103 corresponding to equation 105. Thereby, we obtain the following generating function:

$$B_A = \mathrm{H}^2 + \mathrm{X}_1^2 + \mathrm{X}_2^2 + \mathrm{p}_1\overline{\mathrm{p}}_1 + \mathrm{p}_2\overline{\mathrm{p}}_2 + \mathrm{p}_3\overline{\mathrm{p}}_3 + \mathrm{p}_4\overline{\mathrm{p}}_4. \tag{156}$$

Among the terms appearing in the right-hand side of equation 156, the coefficient 1 of the term $\mathrm{p}_3\overline{\mathrm{p}}_3$ indicates that the term $\mathrm{p}_3\overline{\mathrm{p}}_3$ (corresponding to x^8) is equalized to the inverse term $\overline{\mathrm{p}}_3\mathrm{p}_3$. Thus, the contribution of **36** to the term x^8 (via the term $\mathrm{p}_3\overline{\mathrm{p}}_3$) is counted just once. Hence, the contribution of each balanced 3D-tree is found to be **32** (1)–**36** (1) so as to give the value $B_8^{(A)} = 4$ shown in table 2.

The enumeration result based on equations 108 for $\widehat{B}(x)^{(C)}$ involves another type of irregular specification with respect to the enantiomeric pair (**35** and $\overline{\mathbf{35}}$) because it is again concerned only with carbon contents. Thus, all of the terms vanish in equation 109 in spite of the presence of the enantiomeric pair (**35** and $\overline{\mathbf{35}}$).

The ligand inventories (equations 144–146) are introduced into equation 106 corresponding to equation 108. Thereby, we obtain the following generating function:

$$\begin{aligned}\widehat{B}_C = {} & \frac{1}{2}(\mathrm{p}_1^2 + \overline{\mathrm{p}}_1^2) + \frac{1}{2}(\mathrm{p}_2^2 + \overline{\mathrm{p}}_2^2) + \frac{1}{2}(\mathrm{p}_3^2 + \overline{\mathrm{p}}_3^2) + \frac{1}{2}(\mathrm{p}_4^2 + \overline{\mathrm{p}}_4^2) \\ & - \mathrm{p}_1\overline{\mathrm{p}}_1 - \mathrm{p}_2\overline{\mathrm{p}}_2 - \mathrm{p}_3\overline{\mathrm{p}}_3 - \mathrm{p}_4\overline{\mathrm{p}}_4.\end{aligned} \tag{157}$$

Because the present enumeration result is concerned only with carbon contents, the combined term represented by $\frac{1}{2}(\mathrm{p}_3^2 + \overline{\mathrm{p}}_3^2) - \mathrm{p}_3\overline{\mathrm{p}}_3$ vanishes, as already found in equation 109.

To correct the irregularity of $\widehat{B}(x)^{(C)}$ (equation 108), we use equation 112 for $B(x)^{(C)}$. The coefficient 1 of the term x^8 is in agreement with the presence of one enantiomeric pair of chiral balanced 3D-trees, i.e., **35** and $\overline{\mathbf{35}}$, as collected in table 2 ($B_8^{(C)} = 1$). Thus, the ligand inventories (equations 144–146) are introduced into equation 110 corresponding to equation 112. Thereby, we obtain the following generating function:

$$B_C = \frac{1}{2}(\mathrm{p}_1^2 + \overline{\mathrm{p}}_1^2) + \frac{1}{2}(\mathrm{p}_2^2 + \overline{\mathrm{p}}_2^2) + \frac{1}{2}(\mathrm{p}_3^2 + \overline{\mathrm{p}}_3^2) + \frac{1}{2}(\mathrm{p}_4^2 + \overline{\mathrm{p}}_4^2). \tag{158}$$

Because the present enumeration result is concerned only with carbon contents, the combined term represented by $\frac{1}{2}(\mathrm{p}_3^2 + \overline{\mathrm{p}}_3^2)$ for x^8 corresponds to the enantiomeric pair of **35** and $\overline{\mathbf{35}}$,

The results of the evaluation of balanced 3D-trees are summarized in table 5. The combination of equations 155 and 157 and that of equations 156

Table 5
Evaluation of balanced 3D-trees.

	$B(x)^{(AC)}$	$\widehat{B}(x)^{(A)}$	$\widehat{B}(x)^{(C)}$	$B(x)^{(A)}$	$B(x)^{(C)}$
	B_{AC}	$\widehat{B}_A$	$\widehat{B}_C$	B_A	B_C
$p_3\overline{p}_3$	1	2	−1	1	0
$\frac{1}{2}(p_3^2+\overline{p}_3^2)$	1	0	1	0	1
contribution to x^8	2	2	0	1	1

and 158 give the following equations:

$$B_{AC} = \widehat{B}_A + \widehat{B}_C, \tag{159}$$

$$B_{AC} = B_A + B_C, \tag{160}$$

which correspond to equations 116 and 117. Note that the B_{AC} is obtained by introducing the ligand inventories (equations 144–146) into equation 94 corresponding to equation 96.

4.2. Comments on gross numbers

4.2.1. Gross numbers by $G(x)^{(AC^2)}$

The comparison of the coefficient $140x^8$ in $C(x)^{(AC^2)}$ (equation 49) and the coefficient $139x^8$ in $\widehat{C}(x)^{(AC^2)}$ (equation 29) again exemplifies the effect of the 3D-tree **36** of *meso*-type. The correction by equation 49 is necessary because of the overestimation of $G(x)^{(AC^2)}$ (equation 61), which contains the coefficient $158x^8$.

After introducing equations 144–146 into equation 58, the resulting equation is expanded to give the following generating function:

$$\begin{aligned} G_{AC^2} = \cdots &+ \left(\mathrm{H}^3\mathrm{p}_1 + \mathrm{H}^3\overline{\mathrm{p}}_1\right)\cdots + \left(\mathrm{H}^2\mathrm{X}_1\mathrm{p}_2 + \mathrm{H}^2\mathrm{X}_1\overline{\mathrm{p}}_2\right)\cdots \\ &+ 2\left(\mathrm{HX}_1\mathrm{X}_2\mathrm{p}_3 + \mathrm{HX}_1\mathrm{X}_2\overline{\mathrm{p}}_3\right)\cdots + \left(\mathrm{H}^3\mathrm{p}_4 + \mathrm{H}^3\overline{\mathrm{p}}_4\right)\cdots, \end{aligned} \tag{161}$$

where other terms are omitted so as to leave only necessary terms. Thus, the resulting generating function (equation 161) contains the coefficient 1 of each term $\mathrm{H}^3\mathrm{p}_1$ or $\mathrm{H}^3\overline{\mathrm{p}}_1$ (for **49** or its enantiomer), 1 of each term $\mathrm{H}^2\mathrm{X}_1\mathrm{p}_2$ or $\mathrm{H}^2\mathrm{X}_1\overline{\mathrm{p}}_2$ (for **50** or its enantiomer), and 1 of each term $\mathrm{H}^3\mathrm{p}_4$ or $\mathrm{H}^3\overline{\mathrm{p}}_4$ (for **52** for its enantiomer). The coefficient 2 of the term ($\mathrm{HX}_1\mathrm{X}_2\mathrm{p}_3$ + $\mathrm{HX}_1\mathrm{X}_2\overline{\mathrm{p}}_3$) should be divided into two parts, i.e., the term corresponding to 1 of each term $\mathrm{p}_3\overline{\mathrm{p}}_3$ or $\overline{\mathrm{p}}_3\mathrm{p}_3$ (for the *meso*-3D-tree (**51**)) and 1 of the term p_3^2 or $\overline{\mathrm{p}}_3^2$ (for the chiral 3D-tree (**35** or $\overline{\mathbf{35}}$)). Note that the terms $\mathrm{p}_3\overline{\mathrm{p}}_3$ and $\overline{\mathrm{p}}_3\mathrm{p}_3$ are counted separately, because $\mathrm{p}_3\overline{\mathrm{p}}_3$ and $\overline{\mathrm{p}}_3\mathrm{p}_3$ are regarded irregularly as enantiomers.

Table 6
Evaluation of a 3D-tree of *meso*-type and the related enantiomeric pair.

	Uninuclear	Binuclear	
	$G(x)^{(AC^2)}$	$\widehat{C}(x)^{(AC^2)}$	$C(x)^{(AC^2)}$
	G_{AC^2}	$\widehat{C}_{AC^2}$	C_{AC^2}
$p_3\overline{p}_3$, $\overline{p}_3p_3$	2	1	2
p_3^2, $\overline{p}_3^2$	2	2	2
Contribution to x^8	4	3	4

After introducing equations 146 into 26, the resulting equation is expanded to give the following generating function:

$$\widehat{C}_{AC^2} = \left(X_1p_1 + X_1\overline{p}_1\right)\cdots + \left(X_3p_2 + X_3\overline{p}_2\right)\cdots + \left(X_1p_4 + X_1\overline{p}_4\right)\cdots + \left(p_3^2 + \overline{p}_3^2\right)\cdots + p_3\overline{p}_3\cdots, \tag{162}$$

where other terms are omitted so as to leave only necessary terms. Thus, the resulting generating function (equation 162) contains the coefficient 1 of the term X_1p_1 or $X_1\overline{p}_1$ (for **90** (cf. **49**), total coefficient = 2), 1 of the term X_3p_2 or $X_3\overline{p}_2$ (for **91** (cf. **50**), total coefficient = 2), 1 of the term X_1p_4 or $X_1\overline{p}_4$ (for **93** (cf. **52**), total coefficient = 2), 1 of the term p_3^2 or $\overline{p}_3^2$ (for the enantiomeric pair (**50/$\overline{\mathbf{50}}$**), total coefficient = 2), and 1 of the term $p_3\overline{p}_3$ (for **92** (cf. **51**)).

After introducing equations 146 into 46, the resulting equation is expanded to give the following generating function:

$$C_{AC^2} = \left(X_1p_1 + X_1\overline{p}_1\right)\cdots + \left(X_2p_2 + X_2\overline{p}_2\right)\cdots + \left(X_1p_4 + X_1\overline{p}_4\right)\cdots + \left(p_3^2 + \overline{p}_3^2\right)\cdots + 2p_3\overline{p}_3\cdots, \tag{163}$$

where other terms are omitted so as to leave only necessary terms. Thus, the resulting generating function (equation 163) contains the coefficient 1 of the term X_1p_1 or $X_1\overline{p}_1$ (for **90** (cf. **49**), the total coefficient = 2), 1 of the term X_2p_2 or $X_2\overline{p}_2$ (for **91** (cf. **50**)), 1 of the term X_1p_4 or $X_1\overline{p}_4$ (for **93** (cf. **52**), the total coefficient = 2), 1 of the term p_3^2 or $\overline{p}_3^2$ (for the enantiomeric pair (**50/$\overline{\mathbf{50}}$**), the total coefficient = 2), and 2 of the term $p_3\overline{p}_3$ (for **92** (cf. **51**)).

As summarized in table 6, the difference between $\widehat{C}_{AC^2}$ and C_{AC^2} is the coefficient 1 versus 2 for the term $p_3\overline{p}_3$. This causes the difference between the coefficient $139x^8$ in $\widehat{C}(x)^{(AC^2)}$ (equation 29) and the coefficient $140x^8$ in $C(x)^{(AC^2)}$ (equation 49). Thus the overestimation in G_{AC^2} is cancelled by $C(x)^{(AC^2)}$ (equation 49), i.e., $U_8^{(AC^2)} = G_8^{(AC^2)} - C_8^{(AC^2)} = 158 - 140 = 18$, as collected in table 1.

4.2.2. Gross numbers by $G(x)^{(AC)}$

The gross number given by $G(x)^{(AC)}$ (equation 57) is unnecessary to be corrected, where the uncorrected contaminants evaluated by $C(x)^{(AC)}$ (equation 25) can be used. For example, the coefficients of x^8 in these equations show that $U_8^{(AC)} = G_8^{(AC)} - C_8^{(AC)} = 103 - 89 = 14$, as collected in table 1.

After introducing equations 144–146 into equation 54, the resulting equation is expanded to give the following generating function:

$$G_{AC} = \cdots + \frac{1}{2}\left(\mathrm{H}^3\mathrm{p}_1 + \mathrm{H}^3\overline{\mathrm{p}}_1\right)\cdots + \frac{1}{2}\left(\mathrm{H}^2\mathrm{X}_1\mathrm{p}_2 + \mathrm{H}^2\mathrm{X}_1\overline{\mathrm{p}}_2\right)\cdots + \left(\mathrm{HX}_1\mathrm{X}_2\mathrm{p}_3 + \mathrm{HX}_1\mathrm{X}_2\overline{\mathrm{p}}_3\right)\cdots + \frac{1}{2}\left(\mathrm{H}^3\mathrm{p}_4 + \mathrm{H}^3\overline{\mathrm{p}}_4\right)\cdots, \tag{164}$$

where other terms are omitted so as to leave only necessary terms.

On the other hand, the evaluation of contaminants is conducted by introducing equations 144–146 into equation 22. The resulting equation is expanded to give the following generating function:

$$C_{AC} = \frac{1}{2}\left(\mathrm{X}_1\mathrm{p}_1 + \mathrm{X}_1\overline{\mathrm{p}}_1\right)\cdots + \frac{1}{2}\left(\mathrm{X}_3\mathrm{p}_2 + \mathrm{X}_3\overline{\mathrm{p}}_2\right)\cdots + \frac{1}{2}\left(\mathrm{X}_1\mathrm{p}_4 + \mathrm{X}_1\overline{\mathrm{p}}_4\right)\cdots + \frac{1}{2}\left(\mathrm{p}_3^2 + \overline{\mathrm{p}}_3^2\right)\cdots + \mathrm{p}_3\overline{\mathrm{p}}_3\cdots, \tag{165}$$

where other terms are omitted so as to leave only necessary terms.

The term $\mathrm{HX}_1\mathrm{X}_2\mathrm{p}_3 + \mathrm{HX}_1\mathrm{X}_2\overline{\mathrm{p}}_3$ in equation 164 can be rewritten as $\frac{1}{2}\left(\mathrm{p}_3^2 + \overline{\mathrm{p}}_3^2\right) + \frac{1}{2}\left(\mathrm{p}_3\overline{\mathrm{p}}_3 + \overline{\mathrm{p}}_3\mathrm{p}_3\right)$. Because they correspond to the relevant terms appearing in equation 165, they are canceled during the process of $U_8^{(AC)} = G_8^{(AC)} - C_8^{(AC)} = 103 - 89 = 14$, which corresponds to $G_{AC} - C_{AC}$.

Strictly speaking, the terms $\mathrm{p}_3\overline{\mathrm{p}}_3$ and $\overline{\mathrm{p}}_3\mathrm{p}_3$ in $\frac{1}{2}\left(\mathrm{p}_3\overline{\mathrm{p}}_3 + \overline{\mathrm{p}}_3\mathrm{p}_3\right)$ (equation 164) are regarded as a pair of tentative or hypothetical enantiomers, because the terms $\mathrm{HX}_1\mathrm{X}_2\mathrm{p}_3$ (for $\overline{\mathrm{p}}_3\mathrm{p}_3$) and $\mathrm{HX}_1\mathrm{X}_2\overline{\mathrm{p}}_3$ (for $\mathrm{p}_3\overline{\mathrm{p}}_3$) are different from each other but we can place $\overline{\mathrm{HX}_1\mathrm{X}_2\mathrm{p}_3} = \mathrm{HX}_1\mathrm{X}_2\overline{\mathrm{p}}_3$. On the other hand, the term $\mathrm{p}_3\overline{\mathrm{p}}_3$ (equation 165) is regarded as being achiral. As a result, the successful cancellation described above comes from the methodology in which the term $\frac{1}{2}\left(\mathrm{p}_3\overline{\mathrm{p}}_3 + \overline{\mathrm{p}}_3\mathrm{p}_3\right)$ in the evaluation as uninuclear promolecules is equalized to the term $\mathrm{p}_3\overline{\mathrm{p}}_3$ in the evaluation as binuclear promolecules.

4.3. Partial cycle indices with chirality fittingness

4.3.1. Corrected functions

Although the CI-CF($\mathbf{K}$; $\$_d$) shown in equation 22 (for evaluating $C(x)^{(AC)}$) does not contain the sphericity index a_2, the equations used for correction, i.e., equation 34 for $C(x)^{(A)}$ (equation 36), equation 103 for $B(x)^{(A)}$ (equation 105), and equation 110 for $B(x)^{(C)}$ (equation 112), contain the sphericity index a_2. The

appearance of a_2 should be discussed in a more systematic fashion, although the intuitive explanations have been already mentioned on the basis of geometrical examination.

For this purpose, we apply PCI-CFs (partial cycle indices with chirality fittingness) of the USCI approach [31,32] to the cases of binuclear 3D-trees. By following the procedure described in [31], the PCI-CFs for the subgroups listed in equations 16–20 are obtained as follows:

$$\text{PCI-CF}(\mathbf{K}_1, \$_d) = \frac{1}{4}b_1^2 - \frac{1}{4}b_2 - \frac{1}{4}a_1^2 - \frac{1}{4}c_2 + \frac{1}{2}a_2, \tag{166}$$

$$\text{PCI-CF}(\mathbf{K}_2, \$_d) = \frac{1}{2}b_2 - \frac{1}{2}a_2, \tag{167}$$

$$\text{PCI-CF}(\mathbf{K}_3, \$_d) = \frac{1}{2}a_1^2 - \frac{1}{2}a_2, \tag{168}$$

$$\text{PCI-CF}(\mathbf{K}_4, \$_d) = \frac{1}{2}c_2 - \frac{1}{2}a_2, \tag{169}$$

$$\text{PCI-CF}(\mathbf{K}, \$_d) = a_2, \tag{170}$$

where we use the USCI-CF table and the inverse table of marks for the isomorphic group $\mathbf{C}_{2v}$ (Appendices E.5 and B.5 of Fujita's book [23]).

To obtain equation 34 for $C(x)^{(A)}$ (equation 36), the term c_2 for treating *meso*-type in equation 30 has been replaced by the term a_2. Such unnecessary participation of the *meso*-type can be avoided more rationally as follows. Because 3D-trees of *meso*-type (e.g., p–$\overline{\text{p}}$) belong to $\mathbf{K}_4$ (isomorphic to $\mathbf{C}_s'$), the remaining achiral groups, i.e., $\mathbf{K}_3$ (e.g., X–Y) and $\mathbf{K}$ (e.g., X–X), are used to evaluate achiral contaminants. It follows that the PCI-CFs for these subgroups (equations 168 and 170) are summed up to give the following CI-CF:

$$\begin{aligned}\text{CI-CF}(\mathbf{K}_3 + \mathbf{K}, \$_d) &= \text{PCI-CF}(\mathbf{K}_3, \$_d) + \text{PCI-CF}(\mathbf{K}, \$_d) \\ &= \left(\frac{1}{2}a_1^2 - \frac{1}{2}a_2\right) + a_2 = \frac{1}{2}\left(a_1^2 + a_2\right).\end{aligned} \tag{171}$$

This equation is identical with equation 34 for deriving $C(x)^{(A)}$ (equation 36).

To derive equation 103 for evaluating achiral balanced 3D-trees, the top fraction (1/2) has been introduced rather intuitively. This introduction can be done in a more rational way. Because achiral balanced 3D-trees belong to $\mathbf{K}_4$ (e.g., p—$\overline{\text{p}}$) or $\mathbf{K}$ (e.g., X—X), they are evaluated by the sum of the corresponding PCI-CFs (equations 169 and 170) as follows:

$$\begin{aligned}\text{CI-CF}(\mathbf{K}_4 + \mathbf{K}, \$_d) &= \text{PCI-CF}(\mathbf{K}_4, \$_d) + \text{PCI-CF}(\mathbf{K}, \$_d) \\ &= \left(\frac{1}{2}c_2 - \frac{1}{2}a_2\right) + a_2 = \frac{1}{2}\left(a_2 + c_2\right).\end{aligned} \tag{172}$$

This equation is identical with equation 103 for deriving $B(x)^{(A)}$ (equation 105).

In the above discussion, equation 110 for $B(x)^{(C)}$ (equation 112) has been obtained by the subtraction of equations 103 from 94. Because chiral balanced 3D-trees belong to the subgroup $\mathbf{K}_2$, the same CI-CF can be alternatively obtained by adopting the PCI-CF for the $\mathbf{K}_2$ (equation 167) as follows:

$$\begin{aligned} \text{CI-CF}(\mathbf{K}_2, \$_d) &= \text{PCI-CF}(\mathbf{K}_2, \$_d) \\ &= \frac{1}{2}(b_2 - a_2)\,. \end{aligned} \tag{173}$$

This equation is identical with equation 110 for deriving $B(x)^{(C)}$ (equation 112).

4.3.2. Balanced 3D-trees and adjusted contaminants

In the derivation of equation 94 for $B(x)^{(AC)}$ (equation 96), the top fraction (1/2) has been introduced rather intuitively. This introduction can be done in a more rational way. Because any balanced 3D-tree belongs to $\mathbf{K}_2$ (e.g., p–p or $\overline{\text{p}}$–$\overline{\text{p}}$), $\mathbf{K}_4$ (e.g., p–$\overline{\text{p}}$), or $\mathbf{K}$ (e.g., X–X), they are evaluated by the sum of the corresponding PCI-CFs (equations 167, 169, and 170) as follows:

$$\begin{aligned} \text{CI-CF}(\mathbf{K}_2 + \mathbf{K}_4 + \mathbf{K}, \$_d) &= \text{PCI-CF}(\mathbf{K}_2, \$_d) + \text{PCI-CF}(\mathbf{K}_4, \$_d) + \text{PCI-CF}(\mathbf{K}, \$_d) \\ &= \left(\frac{1}{2}b_2 - \frac{1}{2}a_2\right) + \left(\frac{1}{2}c_2 - \frac{1}{2}a_2\right) + a_2 \\ &= \frac{1}{2}(b_2 + c_2)\,. \end{aligned} \tag{174}$$

This equation is identical with equation 94 for deriving $B(x)^{(AC)}$ (equation 96). The discussion described here is easily extended to general case so as to give the following theorem:

Theorem 8. Any balanced 3D-tree belongs to $\mathbf{K}_2$, $\mathbf{K}_4$, or $\mathbf{K}$.

The PCI-CFs for the subgroups other than those used in equation 174 are summed up to give the following CI-CF:

$$\begin{aligned} \text{CI-CF}(\mathbf{K}_1 + \mathbf{K}_3, \$_d) &= \text{PCI-CF}(\mathbf{K}_1, \$_d) + \text{PCI-CF}(\mathbf{K}_3, \$_d) \\ &= \left(\frac{1}{4}b_1^2 - \frac{1}{4}b_2 - \frac{1}{4}a_1^2 - \frac{1}{4}c_2 + \frac{1}{2}a_2\right) + \left(\frac{1}{2}a_1^2 - \frac{1}{2}a_2\right) \\ &= \frac{1}{4}\left(b_1^2 - b_2 + a_1^2 - c_2\right)\,. \end{aligned} \tag{175}$$

Note that the subgroup $\mathbf{K}_1$ characterizes chiral binuclear promolecules such as X–p, p–q, and p–$\overline{\text{q}}$, while the subgroup $\mathbf{K}_3$ characterizes achiral binuclear promolecules such as X–Y. Obviously, the CI-CF (equation 175) is identical with the one obtained by equation 22 − equation 94 so that it corresponds to equation 123 for evaluating adjusted contaminants $A(x)^{(AC)}$. In fact, the SIs (a_d, c_d,

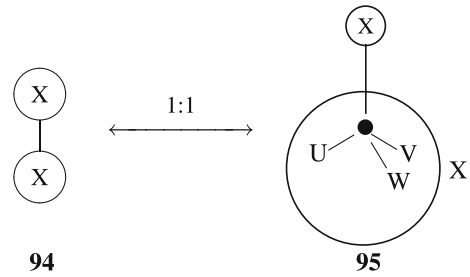

Figure 12. A binuclear promolecule for a balance-edge and the corresponding uninuclear promolecule. Such promolecules as X–X, p–p ($\overline{p}$–$\overline{p}$), and p–$\overline{p}$ exhibit this behavior. They belong to $\mathbf{K}_2$, $\mathbf{K}_4$, or $\mathbf{K}$.

and b_d) in equation 175 is replaced by $a(x^d) - 1$, $c(x^d) - 1$, and $b(x^d) - 1$ to give equation 123. This discussion holds true in general cases, as summarized as a theorem:

Theorem 9. Any 3D-tree as an adjusted contaminant belongs to $\mathbf{K}_1$ or $\mathbf{K}_3$.

In addition, the sum of equations 174 and 175 gives the following CI-CF:

$$\begin{aligned}\text{CI-CF}(\mathbf{K}_1 \cdots \mathbf{K}, \$_d) &= \text{PCI-CF}(\mathbf{K}_1, \$_d) + \text{PCI-CF}(\mathbf{K}_2, \$_d) \\ &\quad + \text{PCI-CF}(\mathbf{K}_3, \$_d) + \text{PCI-CF}(\mathbf{K}_4, \$_d) + \text{PCI-CF}(\mathbf{K}, \$_d) \\ &= \frac{1}{4}\left(b_1^2 + b_2 + a_1^2 + c_2\right), \end{aligned} \tag{176}$$

which is identical with equation 22 for evaluating $C(x)^{(AC)}$.

4.3.3. Yet another proof

Equation 176 combined with theorems 8 and 9 indicates that the contaminants evaluated by $C(x)^{(AC)}$ are categorized into either balanced 3D-trees (belonging to $\mathbf{K}_2$, $\mathbf{K}_4$, or $\mathbf{K}$) or adjusted contaminants (belonging to $\mathbf{K}_1$ or $\mathbf{K}_3$). Thereby, we are able to find a further proof of theorem 7 for $N(x)^{(AC)}$.

The $G(x)^{(AC)}$ of theorem 7 contains the balanced 3D-trees evaluated by $B(x)^{(AC)}$ of theorem 8 as well as the adjusted contaminants evaluated by $A(x)^{(AC)}$ of theorem 9.

Any balanced 3D-tree evaluated by $B(x)^{(AC)}$ of theorem 8 is a binuclear promolecule (**94**), which corresponds to a uninuclear promolecule (**95**) in one-to-one fashion, as shown in figure 12. This means that each balanced 3D-tree is involved in the set of uninuclear promolecules (e.g., **95**) just once without no redundancy. It follows that such balanced 3D-trees should not be deleted.

On the other hand, any adjusted contaminant evaluated by $A(x)^{(AC)}$ of theorem 9 is a binuclear promolecule (**96**), which corresponds to uninuclear promolecules (**97** and **98**) in one-to-two fashion, as shown in figure 13. This means that

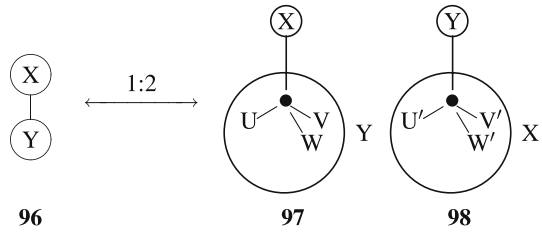

Figure 13. A binuclear promolecule for a slant-edge and the corresponding uninuclear promolecules. Such promolecules as X–Y, A–p (A–$\overline{\text{p}}$), and p–q ($\overline{\text{p}}$–$\overline{\text{q}}$) exhibit this behavior. They belong to $\mathbf{K}_1$ or $\mathbf{K}_3$.

each adjusted contaminant is involved doubly in the set of uninuclear promolecules. It follows that the duplication of the adjusted contaminant should be omitted so as to assure theorem 7.

Similarly, theorem 7 for $N(x)^{(A)}$ can be alternatively proved. As found in the derivation of G_A (equation 147), the $G(x)^{(A)}$ of theorem 7 contains achiral balanced 3D-trees ($\mathbf{K}$) other than those of *meso*-type ($\mathbf{K}_4$) as well as achiral binuclear 3D-trees ($\mathbf{K}_3$). The achiral balanced 3D-trees ($\mathbf{K}$) are contained without no redundancy. Those of *meso*-type ($\mathbf{K}_4$) should be added to avoid the absence of them. The achiral binuclear 3D-trees ($\mathbf{K}_3$) are contained duplicatedly so that the one part should be deleted. Hence, the corresponding adjusted contaminants can be evaluated as follows:

$$\begin{aligned}\text{CI-CF}(\mathbf{K}_3 - \mathbf{K}_4, \$_d) &= \text{PCI-CF}(\mathbf{K}_3, \$_d) - \text{PCI-CF}(\mathbf{K}_4, \$_d) \\ &= \left(\frac{1}{2}a_1^2 - \frac{1}{2}a_2\right) - \left(\frac{1}{2}c_2 - \frac{1}{2}a_2\right) \\ &= \frac{1}{2}\left(a_1^2 - c_2\right). \end{aligned} \tag{177}$$

This equation corresponds to $A(x)^{(A)}$ shown in equation 125.

Theorem 7 for $N(x)^{(C)}$ can be alternatively proved. As found in the derivation of G_C (equation 148), the $G(x)^{(c)}$ of theorem 7 contains chiral binuclear 3D-trees ($\mathbf{K}_1$) as well as achiral balanced 3D-trees of *meso*-type ($\mathbf{K}_4$). The chiral binuclear 3D-trees ($\mathbf{K}_1$) are contained duplicatedly so that the one part should be deleted. The achiral balanced 3D-trees of *meso*-type ($\mathbf{K}_4$) should be deleted. Hence, the corresponding adjusted contaminants can be evaluated as follows:

$$\begin{aligned}\text{CI-CF}(\mathbf{K}_1 + \mathbf{K}_4, \$_d) &= \text{PCI-CF}(\mathbf{K}_1, \$_d) + \text{PCI-CF}(\mathbf{K}_4, \$_d) \\ &= \left(\frac{1}{4}b_1^2 - \frac{1}{4}b_2 - \frac{1}{4}a_1^2 - \frac{1}{4}c_2 + \frac{1}{2}a_2\right) + \left(\frac{1}{2}c_2 - \frac{1}{2}a_2\right) \\ &= \frac{1}{4}\left(b_1^2 - b_2 - a_1^2 + c_2\right). \end{aligned} \tag{178}$$

This equation corresponds to $A(x)^{(C)}$ shown in equation 126.

As an extension of this proof, we are able to develop yet another proof of theorem 6 for $U(x)^{(AC)}$. Between the two uninuclear promolecules (**97** and **98**) corresponding to the binuclear promolecule (**96**), a superior one is defined as follows:

Definition 4. Between the two uninuclear promolecules (**97** and **98**) corresponding to the binuclear promolecule (**96**), the one **97** is defined as being superior to **98**, if the proligand X contains the core selected according to definition 3. On the other hand, the other one **98** is defined as being superior to **97**, if the proligand Y contains the core selected according to definition 3.

1. Suppose that a nuclear is selected as the core of definition 3 for the set of uninuclear promolecules which correspond to an unbalanced 3D-tree. Then, a terminal edge is selected to give the corresponding binuclear promolecule and the two relevant uninuclear promolecules. Between the two relevant uninuclear promolecules, the superior one is saved and the other one is deleted. This procedure is repeated by selecting one of the resulting edges so as to reach the representative promolecule whose nuclear is identical with the selected core. Thereby, the set of uninuclear promolecules is reduced into one unbalanced promolecule (3D-tree) to be counted just once. This means that the finally saved uninuclear promolecule contributes by unit to $U(x) = G(x) - C(x)$ (theorem 6).
   For example, the nuclear of the uninuclear promolecule **14** is selected as a core from the set of **12**–**16** shown in figure 9. Then, after the selection of the edge p–X_1, the uninuclear promolecule **13** is regarded as being superior to the other **12**. Thereby, **12** is deleted by the binuclear promolecule **83** (cf. theorem 5) so that **13** is left for the next step. Next, because **14** is superior to **13**, the inferior one **13** is deleted by the binuclear promolecule **84** so as to give **14** as the representative promolecule.
2. As for a balanced 3D-tree, on the other hand, a terminal edge is also selected to give the corresponding binuclear promolecule and the two relevant uninuclear promolecules. Between the two relevant uninuclear promolecules, the superior one is saved and the other one is deleted (cf. figure 5). This procedure is repeated by selecting one of the resulting edges so as to reach the representative promolecule whose nuclear is identical with either terminal of the balance-edge. The finally saved pair of the uninuclear promolecule and the binuclear promolecule at the one terminal of the balance-edge is identical with the finally saved pair of the uninuclear promolecule and the binuclear promolecule at the other terminal of the balance-edge. Each finally saved pair is cancelled out to give no redundant uninuclear promolecule. No finally saved uninuclear promolecule means that such balanced trees do not contribute to $U(x) = G(x) - C(x)$ (theorem 6).

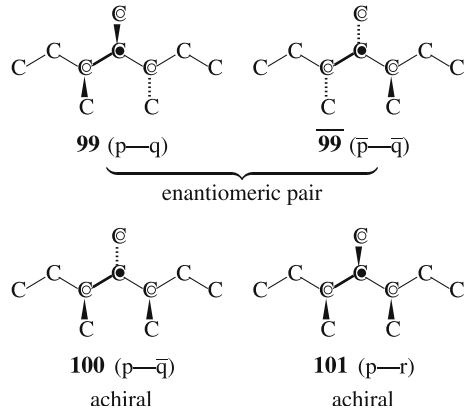

Figure 14. Enantiomeric 3D-trees (**99** and $\overline{\mathbf{99}}$ and diastereomeric 3D-trees (**100** and **101**) related to pseudoasymmetry. Each thick line designates an edge to show the corresponding binuclear promolecule (p–q, etc.).

For example, after the selection of the balance-edge of **32** (figure 5), let us consider the corresponding uninuclear promolecules **37**–**39** shown in figure 10. By selecting the edge p—X_1, the uninuclear promolecule **38** is regarded as being superior to the other **37**. Thereby, **37** is deleted by the binuclear promolecule **87** (cf. theorem 5) so that **38** is left for the next step. Next, because **39** is superior to **38**, the inferior one **38** is deleted by the binuclear promolecule **88** so as to give **39**, which is concerned with the one terminal of the balance-edge of the binuclear promolecule **89**. The pair of the uninuclear promolecule **39** and the binuclear promolecule **89** vanishes to null. This situation holds true for the other terminal of the balance-edge.

It follows that the functional equation $U(x) = G(x) - C(x)$ evaluates the number of unbalanced 3D-trees. That is to say, we have obtained yet another proof of theorem 6.

4.3.4. Pseudoasymmetry

Because two diastereomeric 3D-trees (or alkanes) in a pseudoasymmetric case have been treated properly in terms of Fujita's proligand method, the discussion for figure 13 holds true even for such a pseudoasymmetric case. It is worthwhile, however, to mention some comments on how the present method treats pseudoasymmetric cases.

For example figure 14 depicts enantiomeric 3D-trees (**99** and $\overline{\mathbf{99}}$) and diastereomeric 3D-trees (**100** and **101**), which are related to pseudoasymmetry. The symbols • and ∘ show the core and the substitution positions when each 3D-tree is regarded as a uninuclear 3D-tree. Each thick line designates an edge to show the corresponding binuclear 3D-tree (p—q, etc.).

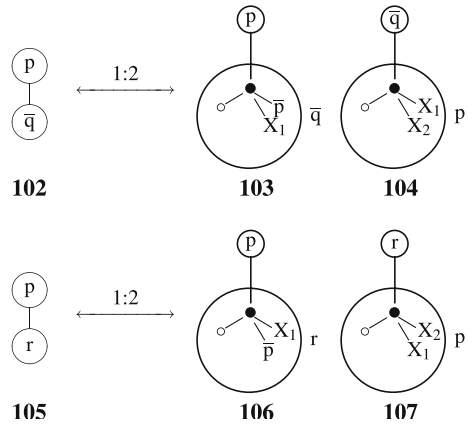

Figure 15. Binuclear promolecules and the corresponding uninuclear promolecules to show a pseudoasymmetric case. The top row shows the 1:2-correspondence for **100** and the bottom row shows the 1:2-correspondence for **101**, where we place p = *R*-CH(CH_3)CH_2CH_3, $\overline{p}$ = *S*-CH(CH_3)CH_2CH_3, X_1 = CH_3, and X_2 = CH_2CH_3; and the other symbols denote the respective remaining parts.

One achiral 3D-tree (**100**) in the pseudoasymmetric case is regarded as a binuclear 3D-tree (p–$\overline{q}$), where one terminal of the edge at issue (thick line) is substituted by the proligand p (= CHX_1X_2) and the other terminal is substituted by the proligand $\overline{q}$ (= $CH\overline{p}X_1$), as shown in **102** (figure 15). When we put a focus on the proligand p (tentatively fixed), we find the corresponding uninuclear 3D-tree (**103**). When we put a focus on the proligand $\overline{q}$ (tentatively fixed), we find the corresponding uninuclear 3D-tree (**104**). It should be noted the core (•) of the uninuclear 3D-tree (**103**) and that of **104** are different from each other and they join the edge of **100** as a binuclear 3D-tree (p–$\overline{q}$).

These two 3D-trees (**103** and **104**) are enumerated separately in terms of uninuclear 3D-trees so as to give redundancy. Hence, the redundancy is deleted by the enumeration in terms of binuclear 3D-trees. Note that the uninuclear 3D-tree (**103**) is counted as an achiral 3D-tree, while the uninuclear 3D-tree (**104**) and the binuclear 3D-tree (**102**) are counted as chiral 3D-trees. Because the binuclear 3D-tree (**102**) as a chiral 3D-tree is not counted as a contaminant for $C(x)^{(A)}$, the contribution of the achiral uninuclear 3D-tree (**103**) to $G(x)^{(A)}$ remains untouched during the application of theorem 7. As a result, the chiral 3D-tree (**100**) in a pseudoasymmetric case is counted just once, giving a correct value of $N(x)^{(A)}$. In contrast, the unnecessary contribution of the chiral uninuclear 3D-tree (**104**) to $G(x)^{(C)}$ is deleted by considering the binuclear 3D-tree (**102**) as a contaminant for $C(x)^{(C)}$ so as to result in no contribution to $N(x)^{(C)}$.

The other achiral 3D-tree (**101**) in a pseudoasymmetric case is regarded as a binuclear 3D-tree (p–r), where one terminal of the edge at issue (thick line) is substituted by the proligand p (= CHX_1X_2) and the other terminal is substituted

by the proligand r (= $CH\overline{p}X_1$), as shown in **105** (figure 15). Note that the proligand r is diastereomeric to the proligand $\overline{q}$ (= $CH\overline{p}X_1$). When we put a focus on the proligand p (tentatively fixed), we find the corresponding uninuclear 3D-tree (**106**). When we put a focus on the proligand r (tentatively fixed), we find the corresponding uninuclear 3D-tree (**107**). These two 3D-trees (**106** and **107**) are enumerated separately in terms of uninuclear 3D-trees so as to give redundancy.

The redundancy for **101** is deleted in a similar way to 3D-tree (**100**). Thus the contribution of the achiral uninuclear 3D-tree (**106**) to $G(x)^{(A)}$ remains untouched, while the unnecessary contribution of the chiral uninuclear 3D-tree (**107**) to $G(x)^{(C)}$ is deleted by considering the binuclear 3D-tree (**105**) as a contaminant for $C(x)^{(C)}$.

5. Comments on earlier accomplishments

The crux of the present work is the concept of sphericity to treat the inner structure of ligands. Hence, it is worthwhile to discuss earlier accomplishments from the viewpoint of the sphericity concept.

The pioneering work by Henze and Blair [13] reported the number of alkanes of a given carbon content, where the alkanes were regarded as graphs, not as 3D-objects. Their work was based on recursive equations, which took no account of the sphericity concept.

Pólya [14] and Pólya and Read [15] evaluated the number of trees as graphs by means of his main theorem (Hauptsatz). Although his discussions covered so-called "steric trees" in terms of the counterpart of equation 58, it took no account of the sphericity concept. In particular, the number of centroidal trees as graphs was evaluated by the following functional equation (equation 2.50 of section 51 [14,15]):

$$s(x) = \frac{x}{24}\left(s(x)^4 + 3s(x^2)^2 + 8s(x)s(x^3) + 6s(x)^2s(x^2) + 6s(x^4)\right). \qquad (179)$$

Obviously, equation 179 is a special case of equation 56 in which we place $s(x^d) = a(x^d) = b(x^d) = c(x^d)$ in the right-hand side. This means the overlooking of the sphericity concept so that Pólya's discussions [14,15] did not pay attention to the stereochemical problems of *meso*-compounds and pseudoasymmetric cases.

Later, Otter [33] reported the enumeration of trees as graphs. His approach was based on the dissimilarity characteristic equation, which provided one of the most elegant solutions on the enumeration of trees as graphs by means of generating functions only. However, his approach also overlooked the sphericity concept and did not pay attention to the stereochemical problems of *meso*-compounds and pseudoasymmetric cases.

More recently, Robinson et al. [19] reported the enumeration of 3D-trees by using the dissimilarity characteristic equation of Ref.33. Their treatment, however, did not take account of the concept of sphericity. For example, they used the following equation:

$$\frac{x}{24}\left(s(x)^4 + 3s(x^2)^2 + 8s(x)s(x^3) + 6a(x)^2 s(x^2) + 6s(x^4)\right), \tag{180}$$

which was derived from equation 179 by geometrical examination (equation 18 of Ref. 19). Obviously, equation 180 is a special case of equation 56 in which we place $s(x^d) = b(x^d) = c(x^d)$. This means that $b(x^d)$ and $c(x^d)$ are mixed up, although $a(x^d)$ is differentiated from $s(x^d) = b(x^d) = c(x^d)$. In other words, the use of equation 180 means the overlooking of the concept of sphericity.

Moreover, the functional equation (equation 22 of Ref. 19):

$$N(x)^{(A)} = \frac{1}{2}\left\{a(x) + xs(x^4) + s(x^2)\right\} - 1, \tag{181}$$

was used even in the case where equation 136 would be required if the sphericity concept was taken into consideration. Because equation 181 is a special case of equation 136 by placing $s(x^d) = c(x^d)$, the two sphericity indices, i.e., $b(x^d)$ (= $s(x^d)$) and $c(x^d)$, are again mixed up.

As a result of the mixing-up of $b(x^d)$ with $c(x^d)$, the stereochemical problems of *meso*-compounds and pseudoasymmetric cases were not treated properly. Thus, the two modes of transitivity ascribed to $c(x^d)$ (e.g., p/$\overline{\text{p}}$ and $\overline{\text{p}}$/p for $d = 2$), which are keys of comprehending the stereochemical problems, were replaced by other two modes of transitivity ascribed to $b(x^d)$ (e.g., p/p and $\overline{\text{p}}/\overline{\text{p}}$ for $d = 2$).

Because the modes of transitivity due to $b(x^d)$ (e.g., p/p and $\overline{\text{p}}/\overline{\text{p}}$) are concerned with chiral ligands, equation 181 means that its right-hand side is evaluated by such modes as p/p and $\overline{\text{p}}/\overline{\text{p}}$ without the compensation of chirality, while its left-hand side aims at evaluating achiral 3D-trees. As a result, both the sides of equation 181 are inconsistent with respect to achirality/chirality, although equation 181 fortunately gave the same results as the present ones using equation 136. This apparent equivalence comes from the fact that the molecular formulas of p and $\overline{\text{p}}$ are equal by considering their carbon contents only.

6. Conclusions

The 3D trees, which are defined as a 3D extension of trees, are enumerated by Fujita's proligand method [16–18], which is based on CI-CFs composed of three kinds of SIs, i.e., a_d for homospheric cycles, c_d for enantiospheric cycles, and b_d for hemispheric cycles. Such 3D-trees are regarded as uninuclear promolecules and enumerated to give the gross number of 3D-trees, which suffers from the redundancy due to contaminants. The 3D-trees are alternatively regarded as binuclear promolecules and enumerated to evaluate the number of such

contaminants. The uninuclear promolecules and the related binuclear ones are compared in terms of the dichotomy between balanced 3D-trees and unbalanced 3D-trees Thereby, the redundancy due to such contaminants is deleted effectively so as to give the net number of 3D-trees, where we take account of such problems as encountered in organic stereochemistry, i.e., *meso*-compounds and pseudoasymmetric cases. The validity of this procedure is proved in three ways, all of which are based on the respective modes of the correspondence between uninuclear promolecules and binuclear ones. In order to enumerate 3D-trees by following this procedure, the CI-CFs are applied to derive functional equations, which are composed of $a(x^d)$, $c(x^d)$, and $b(x^d)$ in accord with the SIs. Thereby, the numbers of 3D-trees or equivalently those of alkanes as stereoisomers are calculated under various conditions and collected up to 20 carbon content in a tabular form. Now, the stereochemical problems (on the number of stereoisomers) by van't Hoff [1] and LeBel [2] and the enumeration problems (on the number of trees) by Cayley [3,4], both initiated in the 1870s, have been solved in a common theoretical framework, which satisfies both chemical and mathematical requirements.

Acknowledgment

We gratefully acknowledge the financial support given to our recent project by the Japan Society for the Promotion of Science: Grant-in-Aid for Scientific Research B (No. 18300033, 2006).

References

[1] J.H. van't Hoff, Arch. Néerlandaises des Sci. Exactes et Nat. 9 (1874) 445–454.
[2] J.A.L. Bel, Bull. Soc. Chim. Fr. (2), 22 (1874) 337–347.
[3] A. Cayley, Philos. Mag. 47 (1874) 444–446.
[4] A. Cayley, Rep. Brit. Assoc. Advance. Sci. 45 (1875) 257–305.
[5] H. Hosoya, Kagaku no Ryoiki, 26 (1972) 989–1001.
[6] D.H. Rouvray, Chem. Soc. Rev. 3 (1974) 355–372.
[7] O.E. Polansky, MATCH Commun. Math. Comput. Chem. 1 (1975) 11–31.
[8] K. Balasubramanian, Chem. Rev. 85 (1985) 599–618.
[9] F. Harary, *Graph Theory* (Addison-Wesley, Reading, 1969).
[10] A.T. Balaban (ed.), *Chemical Applications of Graph Theory* (Academic Press, London, 1976).
[11] N.L. Biggs, E.K. Lloyd, and R.J. Wilson, *Graph Theory 1736–1936* (Oxford University Press, Oxford, 1976).
[12] G. Pólya, R.E. Tarjan, and D.R. Woods, *Notes on Introductory Combinatorics*, (Birkhäuser, Boston, 1983).
[13] H.R. Henze and C.M. Blair, J. Am. Chem. Soc. 53 (1931) 3077–3085.
[14] G. Pólya, Acta Math. 68 (1937) 145–254.
[15] G. Pólya and R.C. Read, *Combinatorial Enumeration of Groups, Graphs, and Chemical Compounds* (Springer-Verlag, New York, 1987).
[16] S. Fujita, Theor. Chem. Acc. 113 (2005) 73–79.

[17] S. Fujita, Theor. Chem. Acc. 113 (2005) 80–86.
[18] S. Fujita, Theor. Chem. Acc. 115 (2006) 37–53.
[19] R.W. Robinson, F. Harary and A.T. Balaban, Tetrahedron, 32 (1976) 355–361.
[20] S. Fujita, Tetrahedron, 47 (1991) 31–46.
[21] S. Fujita, J. Chem. Inf. Comput. Sci. 32 (1992) 354–363.
[22] S. Fujita, Polyhedron, 12 (1993) 95–110.
[23] S. Fujita, *Symmetry and Combinatorial Enumeration in Chemistry* (Springer-Verlag, Berlin-Heidelberg, 1991).
[24] S. Fujita, Theor. Chim. Acta 76 (1989) 247–268.
[25] S. Fujita, J. Math. Chem. 5 (1990) 121–156.
[26] S. Fujita, Bull. Chem. Soc. Jpn. 63 (1990) 203–215.
[27] S. Fujita, MATCH Commun. Math. Comput. Chem. 54 (2005) 251–300.
[28] S. Fujita, MATCH Commun. Math. Comput. Chem. 55 (2006) 5–38.
[29] S. Fujita, MATCH Commun. Math. Comput. Chem. 55 (2006) 237–270.
[30] C. Jordan, J. Reine Angew. Math. 70 (1869) 185–190.
[31] S. Fujita, J. Chem. Inf. Comput. Sci. 40 (2000) 426–437.
[32] S. Fujita, Bull. Chem. Soc. Jpn. 73 (2000) 329–339.
[33] R. Otter, Ann. Math. 49 (1948) 583–599.